Bioorg. Med. Chem. 92 (2023) 117424

Contents lists available at ScienceDirect

Bioorganic & Medicinal Chemistry

journal homepage: www.elsevier.com/locate/bmc

Suramin analogues protect cartilage against osteoarthritic breakdown by increasing levels of tissue inhibitor of metalloproteinases 3 (TIMP-3) in the tissue

Jonathan Green [a,1], Ryan A.J. Tinson [a,b,1], Jacob H.J. Betts [a], Monica Piras [c], Aylin Pelut [a], Dietmar Steverding [a], Stephen P. Wren [c,d], Mark Searcey [b], Linda Troeberg [a,*]

[a] Norwich Medical School, University of East Anglia, Norwich NR4 7UQ, United Kingdom
[b] School of Pharmacy, University of East Anglia, Norwich NR4 7TJ, United Kingdom
[c] Target Discovery Institute, University of Oxford, Oxford OX3 7FZ, United Kingdom
[d] Department of Chemical and Pharmaceutical Sciences, Kingston University, Kingston upon Thames KT1 2EE, United Kingdom

ARTICLE INFO

Keywords:
TIMP-3
Osteoarthritis
Suramin
Low-density lipoprotein receptor-related protein 1
LRP1

ABSTRACT

Osteoarthritis is a chronic degenerative joint disease affecting millions of people worldwide, with no disease-modifying drugs currently available to treat the disease. Tissue inhibitor of metalloproteinases 3 (TIMP-3) is a potential therapeutic target in osteoarthritis because of its ability to inhibit the catabolic metalloproteinases that drive joint damage by degrading the cartilage extracellular matrix. We previously found that suramin inhibits cartilage degradation through its ability to block endocytosis and intracellular degradation of TIMP-3 by low-density lipoprotein receptor-related protein 1 (LRP1), and analysis of commercially available suramin analogues indicated the importance of the 1,3,5-trisulfonic acid substitutions on the terminal naphthalene rings for this activity. Here we describe synthesis and structure–activity relationship analysis of additional suramin analogues using *ex vivo* models of TIMP-3 trafficking and cartilage degradation. This showed that 1,3,6-trisulfonic acid substitution of the terminal naphthalene rings was also effective, and that the protective activity of suramin analogues depended on the presence of a rigid phenyl-containing central region, with *para/para* substitution of these phenyl rings being most favourable. Truncated analogues lost protective activity. The physicochemical characteristics of suramin and its analogues indicate that approaches such as intra-articular injection would be required to develop them for therapeutic use.

1. Introduction

Osteoarthritis is a chronic degenerative joint disease that affects millions of people worldwide [1,2] and has significant socioeconomic impacts on individuals suffering from the disease, as well as broader society. People with osteoarthritis experience joint pain (most commonly in the knee, hip and hand joints), with progressively reduced mobility and quality of life. The disease is caused by alterations in the mechanical environment of the joint, initiated by factors such as ageing or sporting injuries. There are no disease-modifying drugs available that can cure osteoarthritis or halt its progress, and current treatment is limited to pharmacological management of symptoms (e. g. with analgesia or steroids) for early-stage disease and surgical joint replacement for late-stage disease. There is thus considerable interest in developing therapies that can stop disease progression and/or promote healing of the joint.

One approach to treating osteoarthritis is to target enzymes that degrade the cartilage extracellular matrix. Osteoarthritis is

Abbreviations: ADAMTS, adamalysins with disintegrin and thrombospondin domains; CR, complementary regions; DMEM, Dulbecco's modified Eagle's medium; DMMB, dimethylmethylene blue; EtOAc, ethyl acetate; FCS, fetal calf serum; GAG, glycosaminoglycan; IL1β, interleukin 1β; LRP1, low-density lipoprotein receptor-related 1; MMP, matrix metalloproteinase; MTS, [3-(4,5-dimethylthiazol-2-yl)-5-(3-carboxymethoxyphenyl)-2-(4-sulfophenyl)-2H-tetrazolium]; OA, osteoarthritis; PVDF, polyvinylidene fluoride; RAP, receptor-associated protein; RT, room temperature; SDS, sodium dodecyl sulfate; TBS, Tris-buffered saline; TCA, trichloroacetic acid; TIMP-3, tissue inhibitor of metalloproteinases 3.

* Corresponding author at: Norwich Medical School, University of East Anglia, Rosalind Franklin Road, Norwich NR4 7UQ, United Kingdom.
E-mail address: l.troeberg@uea.ac.uk (L. Troeberg).

[1] J Green and RAJ Tinson contributed equally to this work.

https://doi.org/10.1016/j.bmc.2023.117424
Received 19 June 2023; Received in revised form 24 July 2023; Accepted 25 July 2023
Available online 26 July 2023

characterised by increased activity of collagen-degrading matrix metalloproteinases (MMPs) such as MMP-13[3], and related aggrecan-degrading adamalysins with disintegrin and thrombospondin domains (ADAMTSs) such as ADAMTS-5[4,5]. Degradation of the cartilage extracellular matrix by these enzymes impairs the structural integrity of the tissue, leading to progressive joint damage and pain. Metalloproteinase inhibitors have the potential to block cartilage breakdown and promote repair, but attempts to develop such inhibitors are complicated by high homology between metalloproteinase catalytic domains and homeostatic functions of these enzymes in processes such as wound healing and angiogenesis.

An alternative approach is to augment levels of endogenous metalloproteinase inhibitors in cartilage. Tissue inhibitor of metalloproteinases 3 (TIMP-3) is the only one of the 4 human TIMPs that effectively inhibits both MMPs and ADAMTSs, and TIMP-3 has been shown to block cartilage degradation *in vitro*[6] and *in vivo*[7,8]. Levels of TIMP-3 are reduced at the protein level in osteoarthritic cartilage[9], although its mRNA levels are not altered[9,10]. We found that TIMP-3 levels are primarily regulated post-translationally, by endocytosis and lysosomal degradation in chondrocytes via an endocytic scavenger receptor, the low-density lipoprotein receptor-related protein 1 (LRP1)[11,12]. TIMP-3 can also bind to heparan sulfate proteoglycans (HSPGs) in the extracellular matrix[13,14], and this interaction blocks LRP1-mediated uptake and intracellular degradation[15] (Fig. 1). Sulfated compounds like heparin[11], heparan sulfate[15] and calcium pentosan polysulfate[12] can also bind to TIMP-3 and block its interaction with LRP1, thereby increasing extracellular levels of TIMP-3 in cartilage and inhibiting breakdown of the cartilage extracellular matrix.

We showed[16] that TIMP-3 endocytosis by LRP1 can also be inhibited by suramin ($C_{51}H_{40}N_6O_{23}S_6$), a polysulfonated compound used to treat African sleeping sickness caused by *Trypanosome brucei*[17]. Suramin increased levels of TIMP-3 in cartilage and protected against joint damage in a murine model of osteoarthritis[18]. However, therapeutic use of suramin is limited by its systemic toxicity, poor bioavailability and its physicochemical properties. We thus sought to investigate the structure–activity relationship of suramin and its analogues with the view to developing a viable drug candidate to block the endocytosis of TIMP-3 by LRP1.

Previous crystallography, NMR and site-directed mutagenesis studies have shown that multiple LRP1 ligands share a common binding motif, comprised of a pair of basic amino acid residues situated ~ 21 Å apart on the protein surface[19–22]. These basic residues interact with acidic pockets on cysteine-rich complement-type repeats of LRP1[20]. Using site-directed mutagenesis, we confirmed that TIMP-3 shares this common binding mechanism and interacts with LRP1 via pairs of basic residues[23]. Suramin is a C-2 symmetrical compound, substituted with six sulfonic acid groups on the terminal naphthalene rings. We postulated that these highly acidic regions are able to mimic the acidic pockets of LRP1 and drive suramin binding to TIMP-3, and predicted that suramin analogues containing similar clusters of acidic groups separated by ~ 21 Å would similarly bind to TIMP-3 and block its interaction with LRP1. Using 7 commercially available analogues of suramin, we were able to begin probing the suramin/TIMP-3/LRP1 structure–activity relationship (Fig. 2). This showed that analogues shorter than suramin (e. g. NF023 and NF340) or with fewer sulfonic acid groups (e. g. NF110) had lower affinity for TIMP-3 and were less effective at blocking its LRP1-mediated endocytosis and protecting cartilage[16]. NF279 exhibited enhanced affinity for TIMP-3, indicating that the suramin scaffold could be improved upon to achieve enhanced biological activity. We thus sought to synthesise novel analogues of suramin to probe the structure–activity relationship further, and to develop analogues with improved ability to protect cartilage against osteoarthritic breakdown.

2. Results and discussion

2.1. Evaluation of 8-aminonapthalene-1,3,6-trisulfonic acid (NF031)

Suramin and NF279 both have 1,3,5-trisulfonic acid substitutions on their terminal naphthalene rings, but suramin has *meta/meta* substitution of its phenyl rings, while NF279 has *para/para* substitution in this region. This suggests that an extended *para/para*-substitution of the phenyl rings may favour interaction with TIMP-3. To test this hypothesis, we sought to vary the regiochemistry of the phenyl rings. However, the 8-aminonaphthalene 1,3,5-trisulfonic acid building block for both

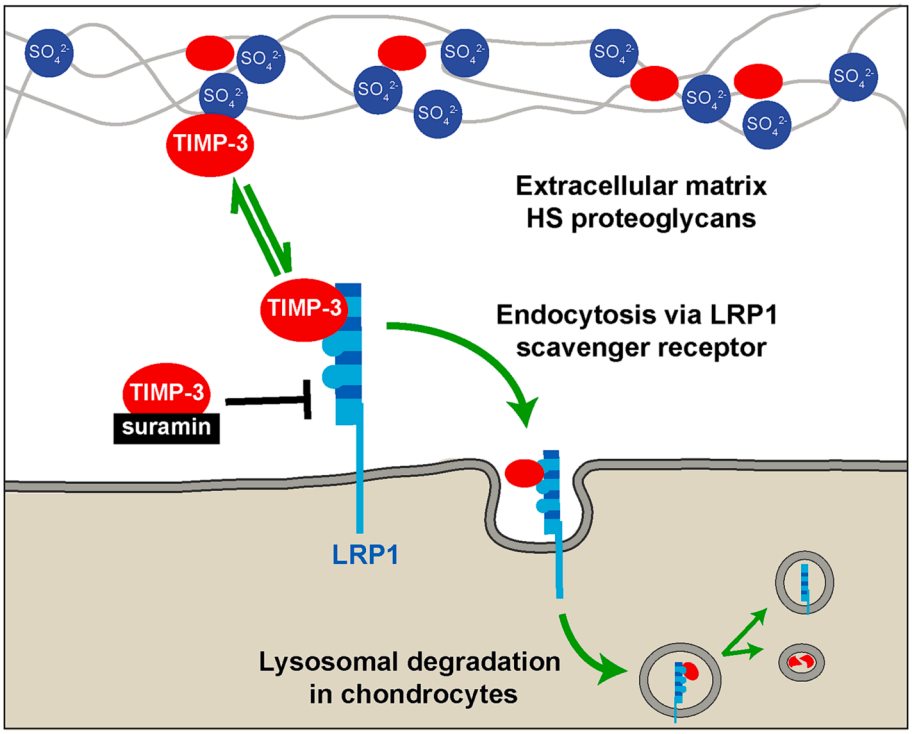

Fig. 1. Suramin increases extracellular levels of TIMP-3 by blocking its endocytosis and lysosomal degradation via LRP1. Sulfated glycosaminoglycans (e. g. heparin, heparan sulfate)[11,15] and polysulfonated molecules (e. g. suramin)[16] bind to an extended basic region on TIMP-3 and so block its interaction with the LRP1 scavenger receptor. By inhibiting TIMP-3 endocytosis and intracellular degradation, suramin thus increases levels of TIMP-3 in the extracellular environment, and protects cartilage against degradation by TIMP-3-target enzymes such as MMP-13 and ADAMTS-5.

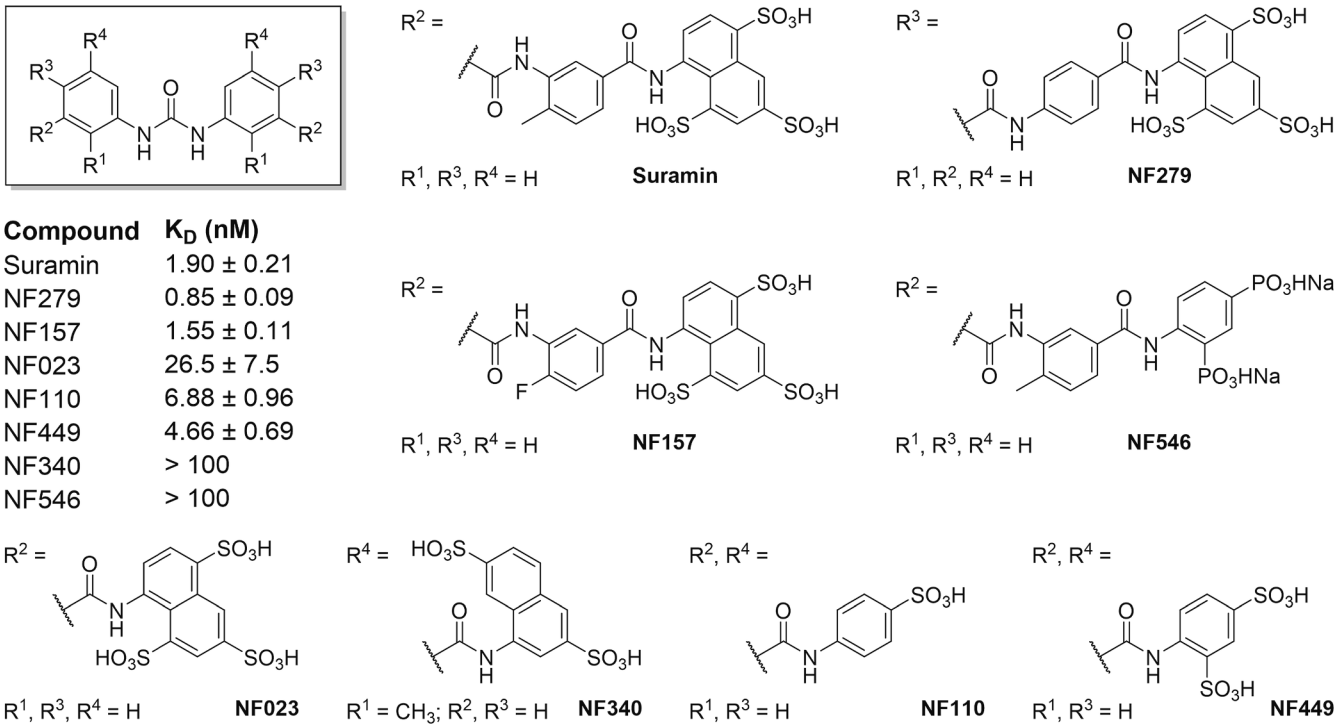

Fig. 2. Structures of suramin and its commercially-available analogues, with K_D values for binding to TIMP-3 determined by ELISA[16].

suramin and NF279 is costly, so we considered a cheaper trisulfonic naphthalene analogues to conduct a structure–activity relationship study. 8-Aminonaphthalene-1,3,6-trisulfonic acid is considerably cheaper, so we used this to synthesise NF031 (Fig. 3 and Scheme 1), which has the *para/para*-substituted linker found in NF279. NF031 has been synthesised previously[24], but to our knowledge is not commercially available. We first compared NF031 to suramin to evaluate the effect of altering the sulfonic acid arrangement.

As we have previously shown[11], levels of TIMP-3 in the conditioned medium of HTB94 chondrosarcoma cells were significantly increased by addition of receptor-associated protein (RAP), an antagonist of ligand binding to the LRP family of endocytic receptors (Fig. 4A). TIMP-3 levels in the media were also significantly increased when cells were treated with 100 μg/mL of suramin or NF031 (Fig. 4A). This indicated that the 8-aminonapthalene-1,3,6-napthalene trisulfonic acid regiochemistry of NF031 was as effective at blocking TIMP-3 endocytosis by LRP1 as the 8-aminonaphthalene 1,3,5-trisulfonic acid arrangement of suramin and NF279.

Shorter precursors of NF031 (compounds **1**–**4**) were ineffective at blocking TIMP-3 endocytosis (Fig. 4B-C), supporting our previous conclusion[16] that two clusters of trisulfonic acid groups were required for binding to an extended basic region of TIMP-3.

2.2. Analysis of phenyl ring regiochemistry structure–activity relationship

Having confirmed that the 8-aminonaphthalene-1,3,6-trisulfonic

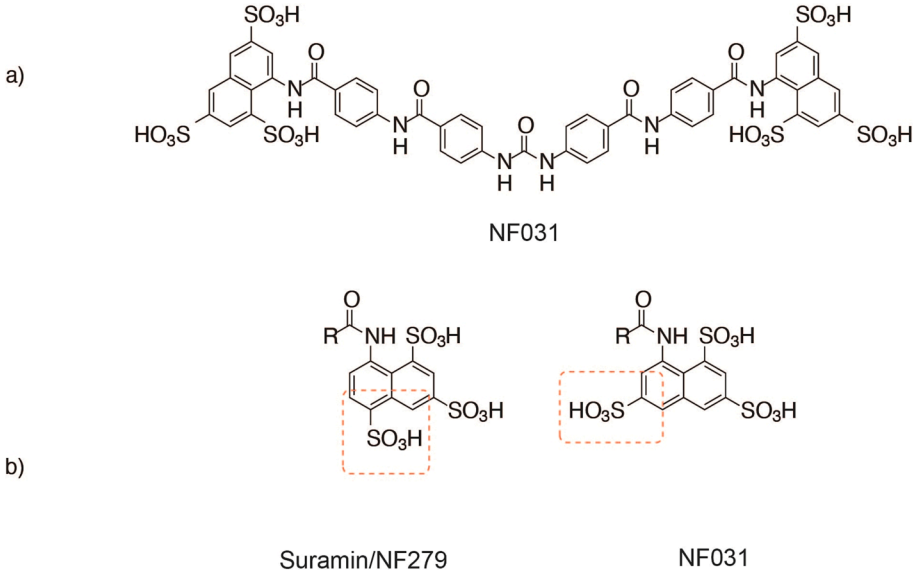

Fig. 3. (A) Structure of NF031. (B) Regiochemistry of sulfonic acid rings in suramin, NF279 and NF031.

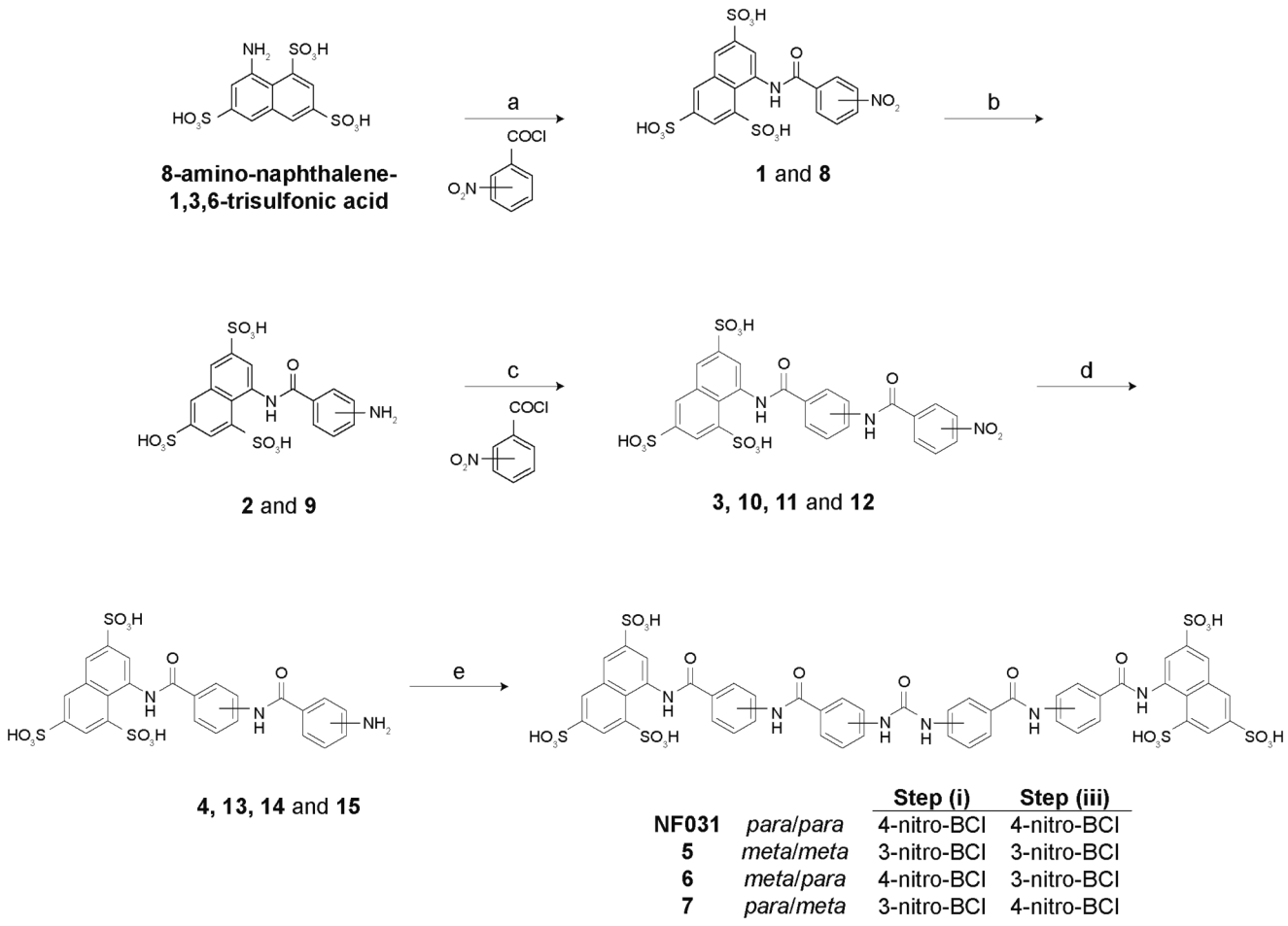

		Step (i)	Step (iii)
NF031	*para/para*	4-nitro-BCl	4-nitro-BCl
5	*meta/meta*	3-nitro-BCl	3-nitro-BCl
6	*meta/para*	4-nitro-BCl	3-nitro-BCl
7	*para/meta*	3-nitro-BCl	4-nitro-BCl

Scheme 1. Synthesis of NF031 and **5**–**7.** (a) $NaHCO_3$ (1 M), 3- or 4-nitro-benzoyl chloride (BCl) (99% for **1**, 96% for **8**); (b) H_2, Pd/C 5 mol%, H_2O (95% for **2**, 62% for **9**); (c) $NaHCO_3$ (1 M), 3- or 4-nitro-benzoyl chloride (82% for **3**, 69% for **10**, 65% for **11**, 87% for **12**); (d) H_2, Pd/C 5 mol%, H_2O (100% for **4**, 76% for **13**, 97% for **14**, 94% for **15**); (e) Triphosgene, $NaHCO_3$ (1 M), pH 6–7, H_2O (45% for **NF031**, 44% for **5**, 39% for **6**, 31% for **7**).

acid arrangement retained activity, we sought to assess regiochemical isomers of NF031 which retained at least 21 Å between the distal naphthalene rings, to ensure that the acidic regions still mimicked the cysteine-rich complement-type repeats of LRP1[20]. We assessed potential structural isomers of NF031 *in silico* (Fig. 5) and found, unsurprisingly, the candidates showing the closest resemblance to NF031 were those containing different regiochemistries of the phenyl rings within the linker e. g. *meta/meta* (**5**), *meta*/para (**6**), and *para/meta* (**7**) compounds.

The synthesis of suramin and its analogues is well documented[25–27] and typically follows an "outside in" approach[28] (Scheme 1). Before adopting this, we tried a strategy that would permit easy functionalisation of our compounds at the latter stages of our synthesis and permit a more convergent route suitable for analysis of the structure–activity relationship. Unfortunately, our initial attempts to synthesise NF031 analogues starting from the formation of the urea via an "inside-out approach" were unsuccessful due to poor solubility of the products. We thus followed an "outside in" synthesis to generate NF031 and its analogues **5**–**7**, which loosely followed the synthesis previously reported by Kassack *et al.*[25]. Initial acylation of 8-amino-naphthalene-1,3,6-trisulfonic acid with 3- or 4-nitro-benzoyl chloride installed the amide group using Schotten-Baumann conditions to give the nitro compounds **1** and **8** in high yields[25]. Hydrogenation of the nitro group afforded compounds **2** and **9**. Then, a second acylation with 3- or 4-nitro-benozyl chloride introduced the second substituted phenyl rings yielding compounds **3** and **10**–**12**, which after hydrogenation over Pd/C gave the amino compounds **4** and **13**–**15**. Urea formation was completed using a triphosgene-mediated reaction to give the desired final compounds **NF031** and **5**–**7** (Scheme 1) in yields of 31–45 %.

All acylation reactions were easily performed by maintaining a pH of 6–7 throughout the reaction, and compound structures were confirmed by their respective *para/meta* splitting patterns in the appropriate ^{1}H NMR spectra. All hydrogenations proceeded smoothly, with products recovered as brown solids after filtering over celite. Confirmation of successful conversion to the amino group was provided by the expected upfield shift in the aromatic protons to a chemical shift in the region of 6.8 ppm due to mesomeric donation of electrons onto the ortho positions. Interpretation of data for the additional acylation and hydrogenation steps was undertaken in a similar manner to confirm the desired synthetic transformation, and in most cases, spectra were superimposed for extra validation. Because of the molecules' C_2-symmetry, urea formation was again confirmed by overlaying the ^{1}H NMR spectra with the precursor amino derivative from the previous step. Additional confirmation of the structures was provided by accurate mass data or elemental analysis.

After establishing that compounds **5**–**7** were not toxic to HTB94 cells (Fig. 6A), we analysed their ability to inhibit TIMP-3 endocytosis via LRP1. HTB94 cells were treated for 36 h with 100 μg/mL of the analogues, and TIMP-3 levels in the conditioned media quantified by immunoblotting. To increase throughput, immunoblotting was performed using a slot blotting apparatus, which allowed for analysis of 24 samples per blot, and which we confirmed gave equivalent quantification to western blotting (Supplementary Figure 1). Samples from cells treated with 100 μg/mL suramin were included on each slot blot to enable relative quantification between blots. NF031 was 30% more

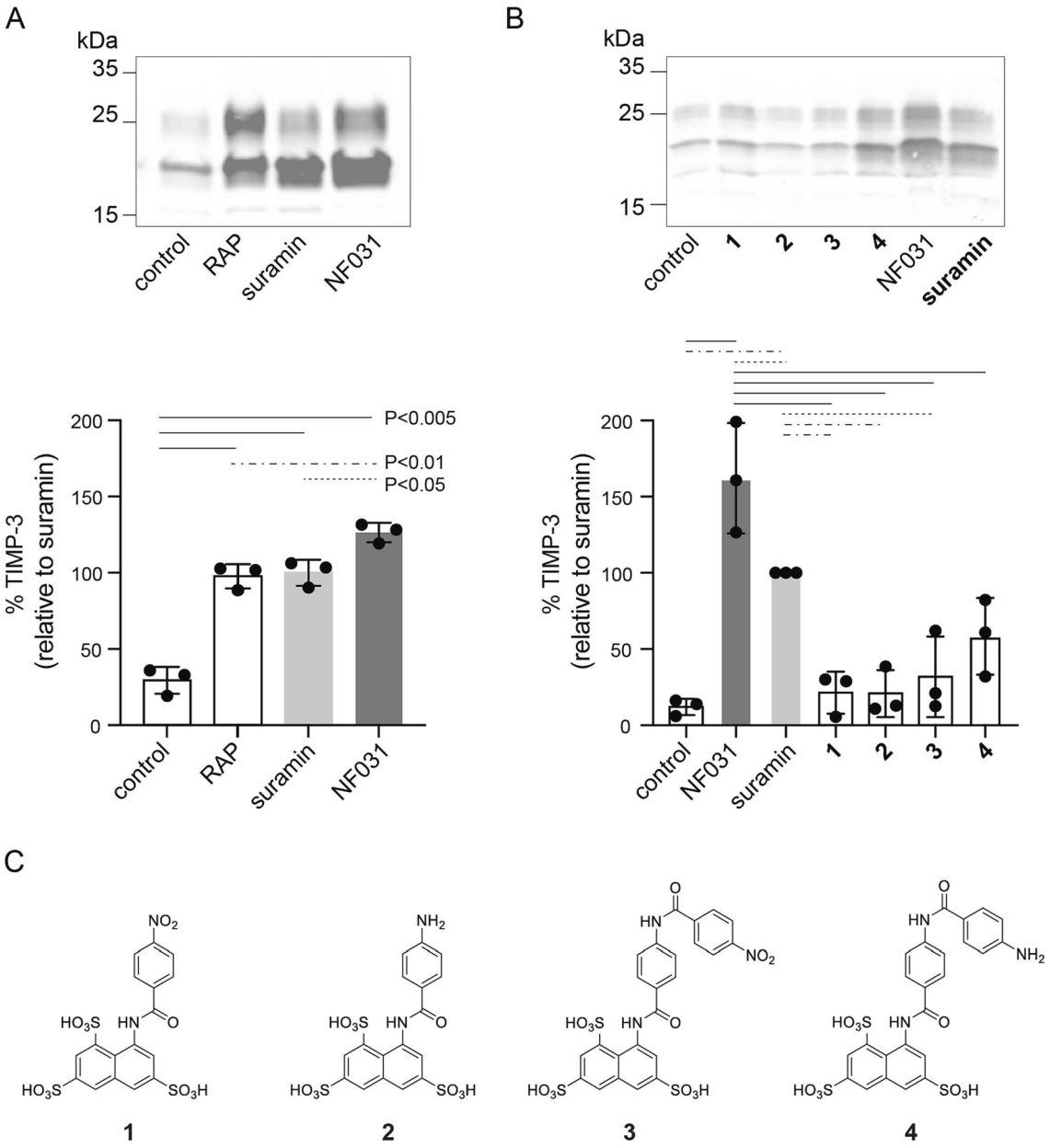

Fig. 4. Suramin, NF031 and RAP increased extracellular TIMP-3 levels. (A) HTB94 chondrosarcoma cells (5x10^5/well) were treated for 36 h with 100 μg/mL suramin or NF031, or 1 μM RAP. TIMP-3 levels in the conditioned media were quantified by western blotting, and expressed relative to TIMP-3 levels in cells treated with 100 μg/mL suramin (n = 3, mean ± SD). (B) HTB94 chondrosarcoma cells (5 × 10^5/well) were treated for 36 h with 100 μg/mL suramin, NF031, or compound **1**–**4**. TIMP-3 levels in the conditioned media were quantified by western blotting as in (A) (n = 3, mean ± SD). (C) Structures of NF031 precursors. P < 0.005 indicated by solid lines; P < 0.01 by dashed lines; and P < 0.05 by dotted lines.

effective than suramin at this concentration, while **5**–**7** were all significantly less effective (~50%) than suramin (Fig. 6B). We then carried out dose-dependency experiments to compare the efficacy of the analogues in more detail (Fig. 6C). Suramin, NF279 and NF031 had similar dose-dependency (EC_{50} values of ~ 20 μg/mL = 15 μM), with NF031 again supporting accumulation of around 30% more TIMP-3 than either suramin or NF279, and **5**–**7** supporting less TIMP-3 accumulation. Comparison of NF031 with **5**–**7** and of NF279 with suramin confirmed that *para/para* regiochemistry of the phenyl rings in the linker region best supported TIMP-3 accumulation.

As we previously observed for suramin[16], NF031 had no effect on mRNA levels of *TIMP3* (Fig. 7A), confirming that it mediated TIMP-3 accumulation post-translationally. Suramin and NF031 also had no significant effects on mRNA levels of *LRP1* (Fig. 7B) and the cartilage-degrading enzymes *ADAMTS4*, *ADAMTS5* and *MMP13* (Supplementary Figure 2). **5**–**7** similarly had minimal effects on expression of these genes, with the exception of **5**, which strongly inhibited expression of *ADAMTS4* at 100 and 200 μg/mL (Supplementary Figure 3).

We then evaluated the ability of NF031 to protect cartilage against the metalloprotease-mediated degradation of aggrecan that characterises osteoarthritis. This was done in the widely-used porcine cartilage explant model, in which the pro-catabolic cytokine interleukin 1β (IL1β) stimulates release of degraded aggrecan fragments into the conditioned media, where they can be quantified using dimethylmethylene blue (DMMB)[29]. IL1β treatment stimulated aggrecan degradation and release into conditioned medium by ~ 4-fold, in accordance with previous reports,[6,16,23] and this degradation was completely inhibited by 100 μg/mL suramin and NF031 (Fig. 8A). Compounds **5**–**7** also inhibited cartilage degradation (Supplementary Figure 4A), but were significantly less effective than NF031 in line with their reduced ability to block TIMP-3

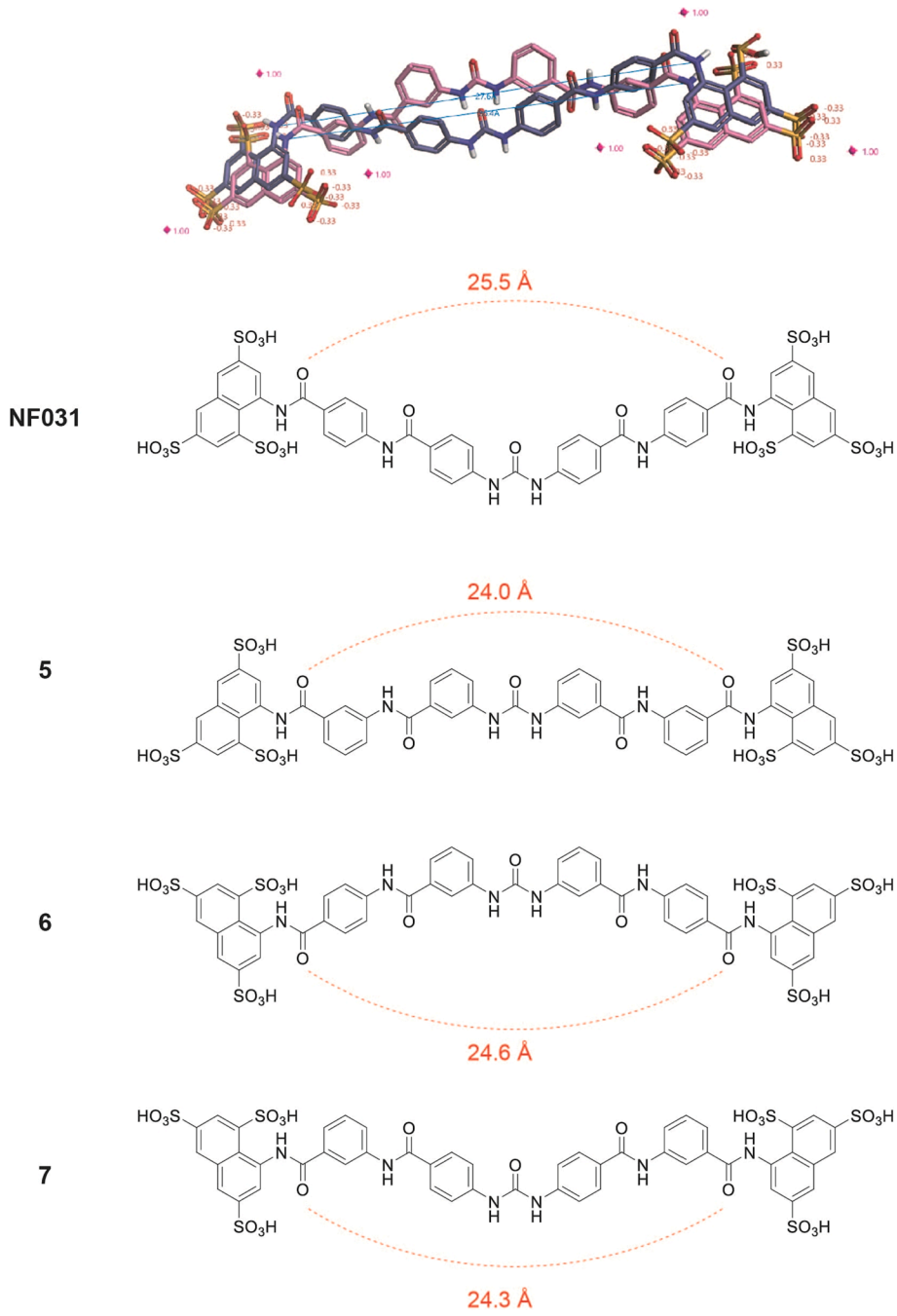

Fig. 5. Comparison of NF031 with its synthesised analogues. NF031 (blue, *para/para*) and its *meta/meta* analogue **5** (pink) were compared using Flare. Structures of the *meta/para* (**6**) and *para/meta* (**7**) analogues are shown for comparison.

endocytosis. None of the analogues exhibited toxicity to chondrocytes at 100 μg/mL, either alone or in combination with IL1β (Fig. 8B and Supplementary Figure 4B).

2.3. Replacement of central phenyl rings with a flexible linker ablated activity

Following analysis of the phenyl ring regiochemistry, we tested the requirement for a rigid linker by installing a tetraethylene linker between the two poly-substituted naphthalene rings of our most promising analogue NF031. Introduction of the tetraethylene linker also facilitated a decrease in molecular weight following Lipinki's rules, an increase in solubility and a shorter synthetic route; all positives in developing new analogues of this type[16]. Computational analysis indicated that compound **16** has comparable length to analogues NF031 and **5**–**7**, and that the tetraethylene linker provided extra flexibility within the linker region but also enough stability to potentially maintain the sulfonic acids in the same location for binding to TIMP-3 (Fig. 9).

Synthesis of compound **16** (Scheme 2) began with the alkylation of tetraethylene glycol di(p-toluenesulfonate) with methyl 4-hydroxybenzoate[30]. Subsequent base hydrolysis gave the di-acid **17**, which was chlorinated using $SOCl_2$ and reacted *in situ* with 1,3,6-napthalene trisulfonic acid to give the novel compound **16**. Analysis of the ^{1}H NMR confirmed the desired product with four singlet peaks for the naphthalene rings at 8.5, 8.4, 7.8 and 7.3 ppm respectively and the expected *para*-substituted splitting pattern of the phenyl rings at 7.7 and 6.9 ppm. Interpretation of the heteronuclear single quantum coherence also depicted a total of six hydrogen environments and nine quaternary

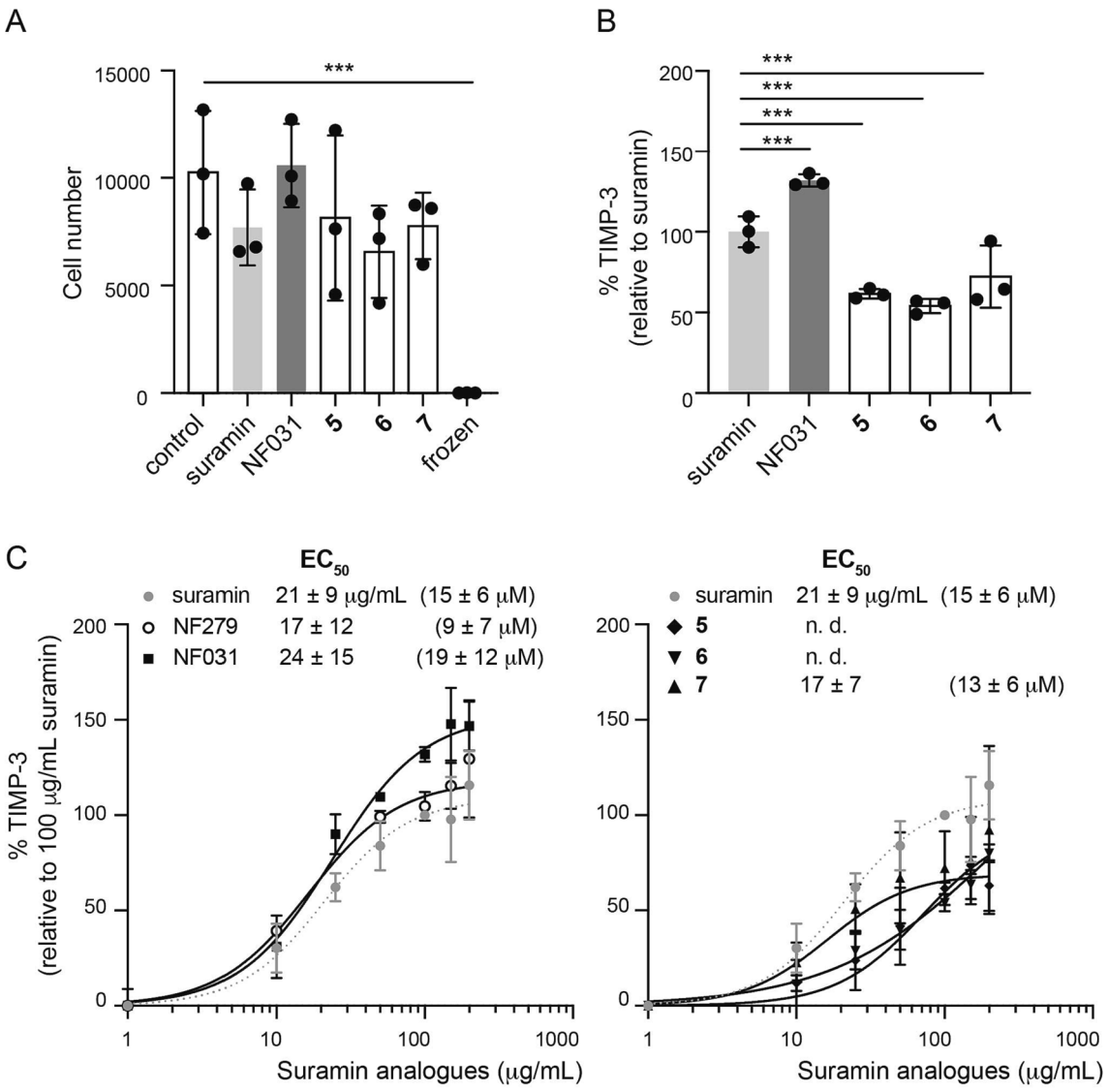

Fig. 6. TIMP-3 endocytosis was most effectively inhibited by NF031. (A) HTB94 chondrosarcoma cells were treated with suramin analogues (100 μg/mL) for 36 h and cell number quantified using the [3-(4,5-dimethylthiazol-2-yl)-5-(3-carboxymethoxyphenyl)-2-(4-sulfophenyl)–2H-tetrazolium] (MTS) assay (n = 3, mean ± SD). As a control for cell death, cells were frozen and thawed twice. (B) HTB94 chondrosarcoma cells were treated with suramin analogues (100 μg/mL) for 36 h. TIMP-3 levels in the conditioned media were quantified by slot blotting, and expressed relative to samples treated with 100 μg/mL suramin (n = 3, mean ± SD). (C) HTB94 chondrosarcoma cells were treated with suramin analogues (0–250 μg/mL) for 36 h. TIMP-3 levels in the conditioned media quantified by slot blotting, and expressed relative to samples treated with 100 μg/mL suramin (n = 3, mean ± SD). EC_{50} values were not determined for **5** and **6** as TIMP-3 accumulation did not plateau within the tested concentration range for these analogues. ***, $P < 0.001$.

centres as expected and was supported by the ^{13}C NMR which contained nineteen carbons for the C_2 symmetric molecule.

Compound **16** was unable to increase levels of TIMP-3 in the media of treated HTB94 chondrosarcoma cells (Fig. 10), indicating that unlike suramin, NF279 and NF031, compound **16** is unable to block TIMP-3 endocytosis by LRP1. This implies that the rigidity provided by the four central phenyl rings (found in NF031 and **5**–**7**) is crucial for stable binding to TIMP-3, and most likely positions the terminal naphthalene rings and their sulfonic acid groups for interaction with the basic residues of TIMP-3.

2.4. Conclusion

TIMP-3 is an effective inhibitor of cartilage degradation both *in vitro* and *in vivo*, and strategies that increase levels of TIMP-3 in cartilage have the potential to be developed into disease-modifying osteoarthritis drugs. We previously showed that suramin is able to increase TIMP-3 levels by inhibiting its endocytosis and intracellular degradation by the LRP1 scavenger receptor, and here we evaluated the structure–activity relationship of additional and novel suramin analogues. This showed that the protective activity of suramin analogues depends on the presence of a rigid phenyl-containing central region, and that *para/para* substitution of these rings (NF031 and NF279) is most favourable. Additionally, we showed that 1,3,6-trisulfonic acid substitution of the terminal naphthalene rings (e.g. NF031) is as effective as 1,3,5-trisulfonic acid substitution (e.g. suramin and NF279).

Truncation of these analogues ablated their protective activity, indicating it is unlikely that a protective molecule obeying Lipinski's rules can be developed from the suramin scaffold. Injection of suramin analogues into affected joints is likely to be a more feasible approach, especially given that a substantial number of osteoarthritis patients already receive intra-articular injections as part of their treatment[31].

TIMP-3 inhibits a broad spectrum of metalloproteinases, and some of these have homeostatic functions in processes such as wound healing. To

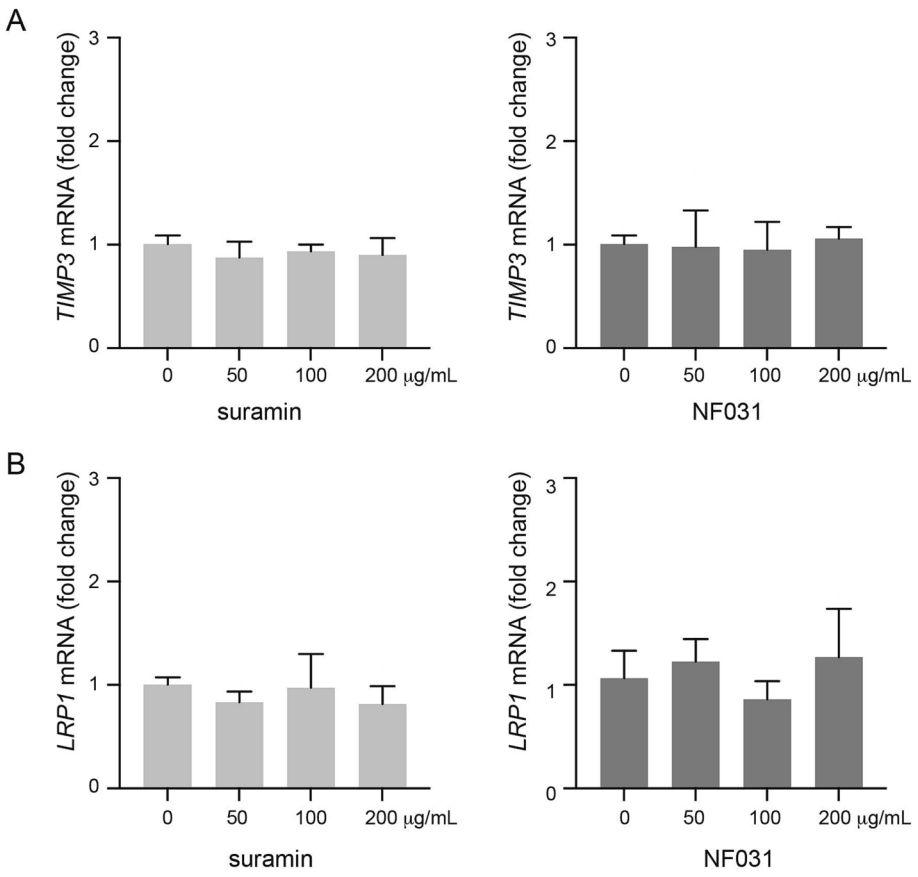

Fig. 7. Suramin and NF031 had no significant effect on mRNA levels of *TIMP3* or *LRP1*. HTB94 chondrosarcoma cells were treated with suramin or NF031 (0–200 μg/mL) for 36 h. RNA was isolated and levels of *TIMP3* (**A**) and *LRP1* (**B**) quantified by RT-qPCR and expressed relative to the housekeeper gene *RN18S1* and untreated cells (n = 3, mean ± SD). There were no significant changes in expression relative to untreated cells.

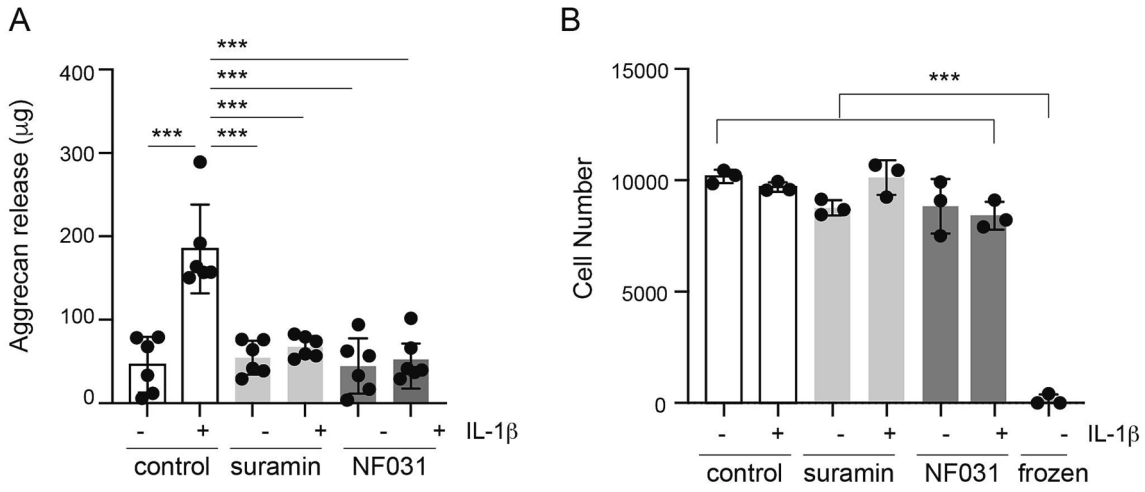

Fig. 8. Suramin and NF031 inhibited cartilage degradation *in vitro*. (A) Porcine cartilage explants were treated with IL1β (10 ng/mL) and suramin or NF031 (100 μg/mL) for 3 days, and aggrecan release into conditioned media quantified using the DMMB assay (n = 3 biological replicates, with 2 technical replicates of each, mean ± SD). (B) Porcine chondrocytes were treated with IL1β (10 ng/mL) and suramin or NF031 (100 μg/mL) for 3 days, and cell number quantified using the MTS assay (n = 3 biological replicates, mean ± SD). As a control for cell death, cells were frozen and thawed twice. There were significantly fewer frozen/thawed cells compared to all other treatments, and no significant differences between other treatments. ***, $P < 0.001$.

limit systemic effects of suramin analogues, it would thus be advantageous to couple them to cartilage-targeting moieties, such as the WYRGRL peptide[32] that has been shown to bind to type II collagen and to increase the half-life of potential therapeutics[33] and imaging probes[34] in joints. Alternatively, the DWRVIIPPRPSA peptide has also been shown to bind to cartilage[35] and to target cargo to the tissue[36]. By increasing retention in cartilage, such approaches would enable use of lower doses with reduced systemic effects.

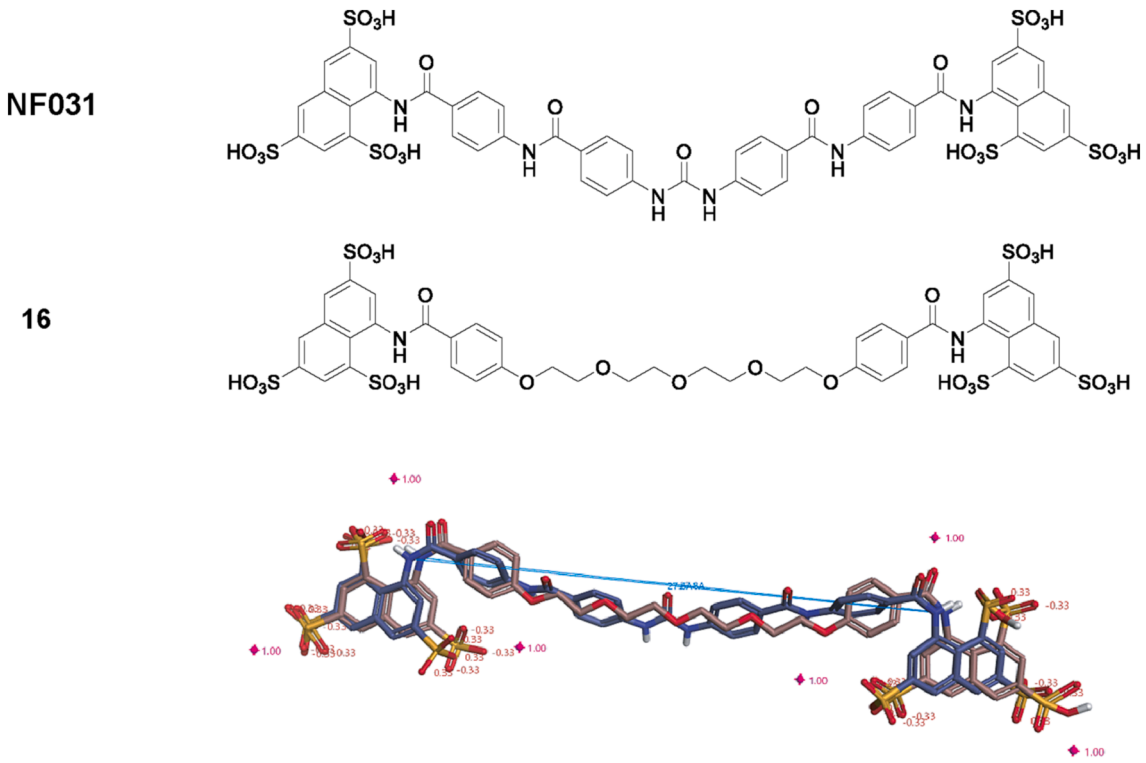

Fig. 9. Comparison of NF031 with compound **16.** NF031 and compound **16** share the same arrangement of 1,3,6-trisulfonic acid substitutions on their terminal naphthalene rings, and computational superimposition of energy minimised NF031 (coloured blue) and **16** shows that the terminal regions can adopt similar conformations. However, NF031 has a rigid phenyl-containing central region, while **16** has a more flexible tetraethylene linker.

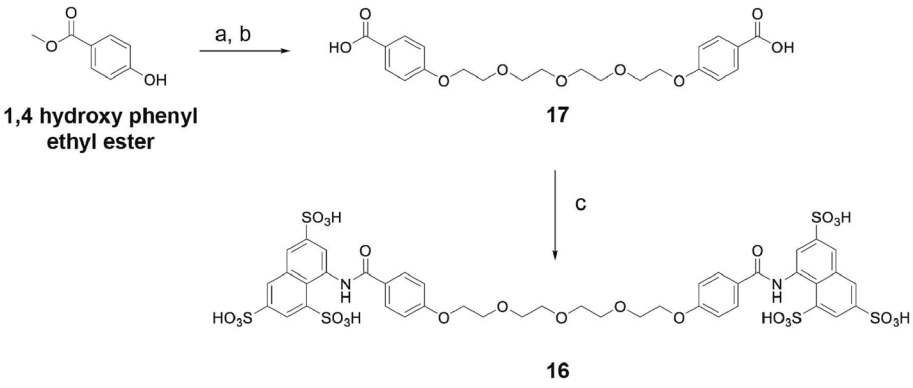

Scheme 2. Synthesis of tetraethyleneglycol linker-containing 1,3,6-trisulfonic acid **16.** (a) K_2CO_3, tetraethylene glycol di(p-toluenesulfonate); (b) LiOH, THF/MEOH, 3 h (43%); (c) $SOCl_2$, 8-amino-1,3,6-napththalene trisulfonic acid (7%).

3. Experimental

3.1. General procedures

All solvents and chemicals were purchased from Acros, TCI, Fluorochem, Alfa Aesar, and Fisher. ^{1}H and ^{13}C NMR spectra were obtained using a Bruker (Ascend) 500 MHz spectrometer and a sample express autosampler. Infrared spectra were obtained on a PerkinElmer ATR spectrometer. Mass spectra were measured by the EPSRC UK National Mass Spectrometry Facility, Swansea, UK using an LTQ Orbitrap XL spectrometer. Melting points were recorded on a Stuart (SIMP3) melting point apparatus. *In silico* analysis of suramin analogues was performed using Flare (Cresset Software, Litlington, Cambridgeshire, UK).

3.2. Chemistry Synthesis of NF031

8-(4-nitrobenzamido)naphthalene-1,3,6-trisulfonic acid (1). 8-Amino-naphthalene-1,3,6-trisulfonic acid disodium salt (2 g, 4.68 mmol) was dissolved in water (10 mL) and the pH was adjusted to 6–7 by adding an aqueous solution of Na_2CO_3 (1 M). To this mixture, a solution of 4-nitro-benzoyl chloride (1.2 g, 6.55 mmol, 1.4 M equivalent) in toluene (10 mL) was added dropwise. The reaction was vigorously stirred for 8 h at room temperature (RT). During this time, the pH was regularly adjusted to 6–7 by adding Na_2CO_3 (1 M). The aqueous phase was acidified to pH 3 (1 M HCl) and extracted with ethyl acetate (EtOAc, 3 × 10 mL). The water was evaporated under reduced pressure at 50 °C and the final product was recovered as a solid yellow powder (2.8 g, 99% yield). Melting point: >350 °C decomposition. ^{1}H NMR (400 MHz, D_2O) δ 8.70 (d, J = 2.0 Hz, 1H), 8.63 (dd, J = 2.0, 0.5 Hz, 1H), 8.49 (d, J = 2.0 Hz, 1H), 8.35 – 8.30 (m, 2H), 8.26 (d, J = 2.0 Hz, 1H), 8.20 – 8.12 (m,

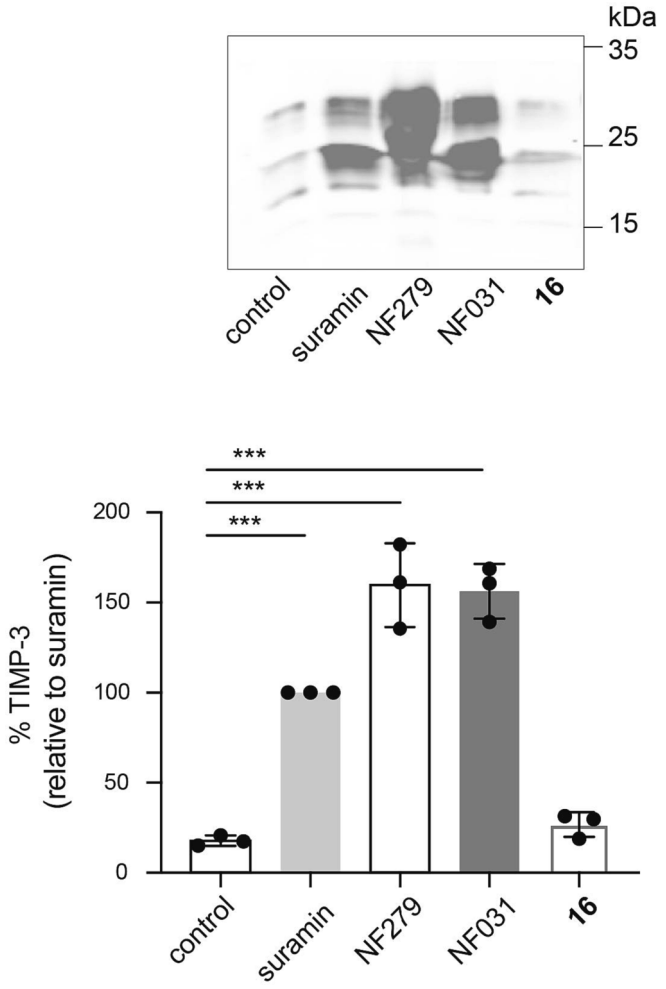

Fig. 10. Compound **16** was unable to support TIMP-3 accumulation. HTB94 chondrosarcoma cells ($5x10^5$/well) were treated for 36 h with 100 μg/mL suramin, NF279, NF031, or **16**. TIMP-3 levels in the conditioned media were quantified by western blotting, and expressed relative to TIMP-3 levels in cells treated with 100 μg/mL suramin (n = 3, mean ± SD).

2H). ^{13}C NMR (101 MHz, D_2O) δ 168.4, 149.7, 141.8, 139.6, 139.5, 138.8, 135.2, 131.8, 131.8, 128.9, 127.0, 127.0, 126.4, 125.9, 123.9. IR νmax/cm^{-1}: 3431 (OH), 1520 (C—H, aromatic sp2 stretch),1350 cm^{-1}. HRMS (nESI-LTQ Orbitrap XL) *m/z*: $[M-2H]^{2-}$ calculated for $C_{17}H_{10}N_2O_{12}S_3$, 205.9988; found, 205.9991.

8-(4-aminobenzamido)naphthalene-1,3,6-trisulfonic acid (2). 8-(4-Nitrobenzamido)naphthalene-1,3,6-trisulfonic acid (**1**) (2.8 g, 5.27 mmol, 1 M equivalent) was dissolved in water (30 mL) and a catalytic amount of Pd/C (ca 55 mg, 0.527 mmol, 0.1 M equivalent) was added. The mixture was vigorously stirred overnight at RT under H_2 (1 standard atmosphere). The mixture was filtered on a pad of celite to remove the catalyst. The water was evaporated under reduced pressure at 50 °C to give the final product as a pale yellow solid (2.4 g, 95% yield). Melting point: >350 °C decomposition. ^{1}H NMR (400 MHz, D_2O) δ 8.69 (d, J = 2.0 Hz, 1H), 8.62 (dd, J = 2.0, 0.5 Hz, 1H), 8.44 (d, J = 2.0 Hz, 1H), 8.18 (d, J = 2.0 Hz, 1H), 7.86 – 7.79 (m, 2H), 6.91 – 6.83 (m, 2H). ^{13}C NMR (101 MHz, D_2O) δ 169.2, 150.7, 141.0, 139.3, 139.0, 135.2, 132.7, 131.9, 129.7, 126.7, 126.2, 126.0, 125.6, 122.9, 115.3. IR νmax /cm^{-1}: 3426 (OH), 1599, 1513 (C—H, aromatic sp2 stretch), 1285 cm^{-1}. HRMS (nESI-LTQ Orbitrap XL) *m/z*: $[M-2H]^{2-}$ calculated for $C_{17}H_{12}N_2O_{10}S_3$, 249.9833; found, 249.9834.

8-[4-(4-nitrobenzamido)benzamido] naphthalene-1,3,6-trisulfonic acid (3). 8-(4-Aminobenzamido)naphthalene-1,3,6-trisulfonic acid (**2**) (2.4 g, 4.7 mmol, 1.0 M equivalent) was dissolved in water (10 mL) and the pH was adjusted to 6–7 by adding an aqueous solution of Na_2CO_3 (1 M). To this mixture, a solution of 4-nitro-benzoyl chloride (1.2 g, 6.55 mmol, 1.4 M equivalent) in toluene (10 mL) was added dropwise. The reaction was vigorously stirred for 8 h at RT. During this time the pH was regularly checked and adjusted to 6–7 by adding Na_2CO_3 (1 M). The water phase was then acidified to pH 3 by adding HCl (1 M) and extracted with EtOAc (3 × 10 mL). Water was evaporated under reduced pressure at 50 °C and the final product was recovered as a yellow solid (2.5 g, 82% yield). Melting point: > 350 °C. This was used for the next step without further purification. ^{1}H NMR (400 MHz, D_2O) δ 8.57 (d, J = 2.0 Hz, 1H), 8.22 (d, J = 2.0 Hz, 1H), 8.04 (s, 2H), 7.78 – 7.70 (m, 2H), 7.41 – 7.29 (m, 6H). ^{13}C NMR (101 MHz, D_2O) δ 166.9, 165.7, 148.2, 140.6, 140.8, 139.2, 138.7, 138.4, 134.6, 131.8, 131.4, 128.6, 128.2, 126.4, 125.4, 124.2, 124.4, 122.6, 120.1. IR νmax/cm^{-1}: 3470 (OH), 1658, 1597, 1524 (C—H, aromatic sp2 stretch), 1280 cm^{-1}. HRMS (nESI-LTQ Orbitrap XL) *m/z*: $[M-3H]^{3-}$ calculated for $C_{24}H_{14}N_3O_{13}S_3$, 215.9902; found, 215.9903.

8-[4-(4-aminobenzamido)benzamido] naphthalene-1,3,6-trisulfonic acid (4). 8-[4-(4-Nitrobenzamido)benzamido]naphthalene-1,3,6-trisulfonic acid (**3**) (2.5 g, 3.84 mmol, 1.0 M equivalent) was dissolved in water (30 mL) and a catalytic amount of Pd/C (ca 50 mg, 0.38 mmol, 0.1 M equivalent) was added. The mixture was vigorously stirred overnight at RT under H_2 (1 standard atmosphere). The mixture was filtered on a pad of celite to remove the catalyst and the water was evaporated under reduced pressure at 50 °C to give the product as a pale yellow solid (2.4 g, 100% yield). Melting point: >350 °C. ^{1}H NMR (400 MHz, D_2O) δ 8.70 (d, J = 2.0 Hz, 1H), 8.43 (d, J = 2.0 Hz, 1H), 8.18 (s, 2H), 7.84 – 7.76 (m, 2H), 7.56 – 7.47 (m, 2H), 7.13 – 7.05 (m, 2H), 6.27 – 6.19 (m, 2H). ^{13}C NMR (101 MHz, D_2O) δ 167.6, 167.3, 148.8, 141.4, 140.5, 138.9, 138.7, 134.9, 131.9, 131.9, 128.8, 128.6, 128.2, 126.6, 126.4, 124.9, 124.5, 122.5, 120.3, 115.6. IR νmax /cm^{-1}: 3457 (OH), 1658, 1598, 1525 (C—H, aromatic sp2 stretch), 1280 cm^{-1}. HRMS (nESI-LTQ Orbitrap XL) *m/z*: $[M-3H]^{3-}$ calculated for $C_{24}H_{16}N_3O_{11}S_3$, 205.9988; found, 205.9991.

8-(4-(4-[({4-[(4-{hydroxy[(3,6,8-*trisulfonaphthalen*-1-*yl*) *amino*] methyl)phenyl)carbamoyl] phenyl)carbamoyl)amino] benzamido)benzamido)naphthalene-1,3,6-trisulfonic acid (NF031). 8-[4-(4-Nitrobenzamido)benzamido]naphthalene-1,3,6-trisulfonic acid (**4**) (256 mg, 0.4 mmol) was dissolved in water (3 mL) and the pH was adjusted to 6–7 by adding an aqueous solution of Na_2CO_3 (1 M). To this mixture, a solution of triphosgene (60 mg, 0.2 mmol) in toluene (3 mL) was added dropwise. The reaction was vigorously stirred for 8 h at RT. During this time the pH was regularly checked and adjusted to 6–7 by adding Na_2CO_3 (1 M). The water phase was extracted with EtOAc (3 × 5 mL). Water was then evaporated under vacuum at 50 °C affording a pale yellow solid (230 mg, 45% yield). Melting point: >350 °C. ^{1}H NMR (400 MHz, DMSO-d_6) δ 12.45 (s, 1H), 10.44 (s, 1H), 10.16 (s, 1H), 8.59 (d, J = 1.9 Hz, 1H), 8.49 (d, J = 1.8 Hz, 1H), 8.23 – 8.13 (m, 3H), 8.05 – 7.91 (m, 6H), 7.67 (d, J = 8.4 Hz, 2H). ^{13}C NMR (101 MHz, DMSO-d_6) δ 165.8, 165.3, 152.9, 145.5, 143.7, 143.5, 142.5, 142.0, 134.9, 133.8, 130.6, 129.5, 129.2, 128.4, 128.0, 126.6, 122.9, 122.6, 119.6, 117.4, 40.5, 40.3, 40.1, 39.9, 39.7, 39.5, 39.3. IR νmax /cm^{-1}: 3450 (OH), 1658, 1603, 1525 (C—H, aromatic sp2 stretch), 1352 cm^{-1}. HRMS (nESI-LTQ Orbitrap XL) *m/z*: $[M-5H]^{5-}$ calculated for $C_{49}H_{31}N_6O_{23}S_6$, 252.5958; found, 252.5960.

*3.2.1. Synthesis of **5***

8-(3-nitrobenzamido)naphthalene-1,3,6-trisulfonic acid (8). 8-Amino-naphthalene-1,3,6-trisulfonic acid disodium salt (2 g, 4.68 mmol, 1.0 M equivalent) was dissolved in water (10 mL) and the pH was adjusted to 6–7 by adding an aqueous solution of Na_2CO_3 (1 M). To this mixture, a solution of 3-nitro-benzoyl chloride (1.2 g, 6.55 mmol, 1.4 M equivalent) in toluene (10 mL) was added dropwise. The reaction was vigorously stirred for 8 h at RT. During this time the pH was regularly adjusted to 6–7 by adding Na_2CO_3 (1 M). The water layer was then acidified by adding HCl 1 M (pH 3) and extracted with EtOAc (3 × 30

mL). The water was then evaporated under reduced pressure at 50 °C to give the final product as a solid yellow powder (2.4 g, 96% yield). ^{1}H NMR (400 MHz, D_2O) δ 8.71 (ddd, J = 7.0, 4.7, 2.0 Hz, 2H), 8.61 (dd, J = 5.4, 2.1 Hz, 1H), 8.45 – 8.40 (m, 1H), 8.33 – 8.27 (m, 2H), 8.20 – 8.15 (m, 1H), 7.57 – 7.50 (m, 1H). ^{13}C NMR (101 MHz, D_2O) δ 167.1, 147.7, 141.1, 139.5, 138.8, 135.2, 134.2, 131.8, 131.7, 130.2, 129.5, 126.9, 126.9, 126.7, 125.69, 123.6, 122.9. IR νmax /cm^{-1}: 3451 (OH), 1649, 1527 (C—H, aromatic sp2 stretch) and 1351 cm^{-1}. HRMS M = $C_{17}H_{12}N_2O_{12}S_3$ $[M-H]^{(-)}$ expected 530.9480; found 530.9508.

8-(3-aminobenzamido)naphthalene-1,3,6-trisulfonic acid (9). To 8-(3-Nitrobenzamido)naphthalene-1,3,6-trisulfonic acid (**8**) (2.4 g, 1.0 M equivalent), Pd/C (ca. 100 mg, 0.1 M equivalent) was added and the round bottomed-flask was evacuated/flushed with N_2 three times. Water (10 mL) was added to the flask and the same procedure was performed with evacuation/filling with H_2. The reaction was left overnight to stir at atmospheric pressure under H_2. The reaction was filtered over a pad of celite and concentrated under reduced pressure to give a yellow solid (1.4 g, 62% yield). ^{1}H NMR (400 MHz, D_2O) δ 8.72 (d, J = 2.0 Hz, 1H), 8.64 (d, J = 2.0 Hz, 1H), 8.48 (d, J = 2.0 Hz, 1H), 8.25 (d, J = 2.0 Hz, 1H), 7.44 – 7.34 (m, 2H), 7.29 (t, J = 7.8 Hz, 1H), 6.99 (ddd, J = 8.0, 2.5, 1.0 Hz, 1H). ^{13}C NMR (101 MHz, D_2O) 169.9, 146.6, 141.0, 139.4, 139.0, 135.2, 134.6, 132.3, 131.8, 129.8, 126.8, 126.7, 126.0, 125.8, 120.3, 118.6, 115.1. IR νmax /cm^{-1}: 3410 (OH), 1640, 1525- (C—H, aromatic sp2 stretch). HRMS M = $C_{17}H_{14}N_2O_{10}S_3$ $[M-H]^{(-)}$ expected 500.9738; found 500.9742.

8-[3-(3-nitrobenzamido)benzamido] naphthalene-1,3,6-trisulfonic acid (10). To 8-(3-Aminobenzamido)naphthalene-1,3,6-trisulfonic acid **(9)** (200 mg, 0.4 mmol, 1.0 M equivalent), water (2 mL) was added and the pH was adjusted to 6–7. To this, 3-nitro benzoyl chloride (105 mg, 0.55 mmol, 1.4 M equivalent) dissolved in toluene (2 mL) was added. The reaction was then stirred vigorously over a period of 8 h while the pH was continually adjusted to pH 6–7. The toluene layer was removed and the aqueous layer was acidified to pH 3 and extracted with EtOAc (3 × 10 mL). The remaining aqueous layer was evaporated to dryness to give the product (180 mg, 69% yield). ^{1}H NMR (400 MHz, D_2O) δ 8.33 (d, J = 1.8 Hz, 1H), 7.92 (s, 1H), 7.86 (s, 1H), 7.76 (s, 1H), 7.68 (s, 1H), 7.48 (d, J = 7.5 Hz, 1H), 7.34 (d, J = 7.3 Hz, 1H), 7.11 (d, J = 7.8 Hz, 1H), 6.92 (d, J = 7.7 Hz, 1H), 6.80 (t, J = 7.7 Hz, 1H), 6.60 (t, J = 7.8 Hz, 1H). ^{13}C NMR (101 MHz, D_2O) δ 166.2, 164.6, 147.6, 145.6, 140.4, 139.1, 138.0, 137.9, 137.6, 134.5, 133.7, 133.2, 132.5, 131.7, 131.3, 129.0, 128.3, 126.3, 125.0, 123.8, 123.0, 122.6, 121.4, 118.9. IR νmax /cm^{-1}: 3451 (OH), 1654, 1595 and 1527 (C—H, aromatic sp2 stretch). HRMS (nESI-LTQ Orbitrap XL) *m/z*: $[M-3H]^{3-}$ calculated for $C_{24}H_{14}N_3O_{13}S_3$, 215.9902; found, 215.9905.

8-[3-(3-aminobenzamido)benzamido] naphthalene-1,3,6-trisulfonic acid (13). 8-[3-(3-Nitrobenzamido)benzamido]naphthalene-1,3,6-trisulfonic acid (**10**) (180 mg, 0.276 mmol, 1.0 M equivalent) was dissolved in water (5 mL) and a catalytic amount of Pd/C (ca 30 mg, 0.1 M equivalent) was added. The mixture was vigorously stirred overnight at RT under H_2 (1 standard atmosphere). The mixture was filtered on a pad of celite to remove the catalyst. The water was evaporated under reduced pressure at 50 °C and the final product was recovered as a fine pale brown powder. (130 mg, 76% yield). ^{1}H NMR (400 MHz, D_2O) δ 8.66 (s, 1H), 8.54 (s, 1H), 8.38 (s, 1H), 8.21 (s, 1H), 8.05 (s, 1H), 7.74 (d, J = 7.8 Hz, 1H), 7.65 (d, J = 8.1 Hz, 1H), 7.44 (t, J = 8.0 Hz, 1H), 7.04 – 6.93 (m, 3H), 6.69 (d, J = 7.5 Hz, 1H). ^{13}C NMR (101 MHz, D_2O) δ 168.5, 168.4, 146.2, 140.8, 139.2, 138.8, 137.5, 137.5, 135.1, 134.0, 132.1, 131.8, 129.5, 129.4, 126.7, 126.4, 125.6, 125.4, 125.1, 124.5, 120.6, 119.8, 117.9, 114.5. IR νmax /cm^{-1}: 3401 (OH), 1652, 1588 and 1538 (C—H, aromatic sp2 stretch). HRMS (nESI-LTQ Orbitrap XL) *m/z*: $[M-3H]^{3-}$ calculated for $C_{24}H_{16}N_3O_{11}S_3$, 205.9990; found, 2059988.

8-{3-[3-([3-((3-[(3,6,8-trisulfonaphthalen-1-yl)carbamoyl] phenyl)carbamoyl)phenyl] carbamoyl)amino)benzamido] benzamido}naphthalene-1,3,6-trisulfonic acid (5). 8-[3-(3-Aminobenzamido)benzamido]naphthalene-1,3,6-trisulfonic acid **(13)** was dissolved in water (3 mL) and the pH was adjusted to 6–7 by adding an aqueous solution of Na_2CO_3 (1 M). To this mixture, a solution of triphosgene (60 mg, 0.2 mmol) in toluene (3 mL) was added dropwise. The reaction was vigorously stirred for 8 h at RT, with the pH regularly adjusted to 6–7 by adding Na_2CO_3 (1 M). The water phase was extracted with EtOAc (3 × 10 mL). Water was evaporated under vacuum at 50 °C affording a pale yellow solid. (224 mg, 44%). Melting point: >350 °C. ^{1}H NMR (400 MHz, D_2O) δ 8.53 (s, 1H), 8.51 (s, 1H), 8.38 (s, 1H), 8.18 (s, 1H), 8.12 (s, 1H), 7.83 (s, 1H), 7.76 (d, J = 8.0 Hz, 1H), 7.67 (d, J = 7.6 Hz, 1H), 7.34 (t, J = 7.9 Hz, 1H), 7.27 (s, 1H), 7.17 (t, J = 7.7 Hz, 1H), 7.03 (d, J = 7.8 Hz, 1H). ^{13}C NMR (101 MHz, D_2O) δ 168.6, 167.7, 153.6, 140.9, 139.6, 138.8, 137.9, 137.6, 135.5, 133.6, 133.6, 132.2, 131.9, 129.9, 129.3, 126.6, 126.8, 125.5, 125.7, 124.44, 122.66, 122.31, 120.02, 117.19. IR νmax /cm^{-1}: 3447 (OH), 1645, 1591 and 1529 (C—H, aromatic sp2 stretch). HRMS (nESI-LTQ Orbitrap XL) *m/z*: $[M-5H]^{5-}$ calculated for $C_{49}H_{31}O_{23}N_6S_6$, 252.5958; found, 252.5962.

3.2.2. Synthesis of 6

8-[4-(3-nitrobenzamido)benzamido] naphthalene-1,3,6-trisulfonic acid (11). 8-(4-Aminobenzamido)naphthalene-1,3,6-trisulfonic acid (**2**) (240 mg, 0.47 mmol, 1.0 M equivalent) was dissolved in water (3 mL) and the pH was adjusted to 6–7 by adding an aqueous solution of Na_2CO_3 (1 M). To this mixture, a solution of 3-nitro-benzoyl chloride (120 mg, 0.65 mmol, 1.4 M equivalent) in toluene (3 mL) was added dropwise. The reaction was vigorously stirred for 8 h at RT. During this time the pH was regularly checked and adjusted to 6–7 by adding Na_2CO_3 (1 M). The water phase was acidified to pH 3 by adding HCl (1 M) and extracted with EtOAc (3 × 10 mL). The water was evaporated under reduced pressure at 50 °C to give the final product as a yellow solid (200 mg, 65% yield). Melting point: >350 °C. ^{1}H NMR (400 MHz, D_2O) δ 8.64 (d, J = 2.0 Hz, 1H), 8.43 (d, J = 2.0 Hz, 1H), 8.25 – 8.08 (m, 3H), 7.89 (d, J = 8.7 Hz, 3H), 7.84 – 7.72 (m, 1H), 7.58 (d, J = 8.6 Hz, 2H), 7.13 (t, J = 8.0 Hz, 1H). ^{13}C NMR (101 MHz, D_2O) δ 167.1, 165.3, 146.5, 140.9, 140.7, 139.3, 138.5, 134.8, 134.1, 133.3, 131.9, 131.5, 129.3, 128.7, 128.6, 126.6, 126.5, 125.6, 124.3, 124.2, 121.9, 120.2. IR νmax /cm^{-1}: 3461 (OH), 1596, 1525 (C—H, aromatic sp2 stretch) cm^{-1}.HRMS (nESI-LTQ Orbitrap XL) *m/z*: $[M-2H]^{2-}$calculated for $C_{24}H_{15}N_3O_{13}S_3$, 324.4889; found, 324.4884.

8-[4-(3-aminobenzamido)benzamido] naphthalene-1,3,6-trisulfonic acid (14). 8-[4-(3-Nitrobenzamido)benzamido]naphthalene-1,3,6-trisulfonic acid (**11**) (200 mg, 0.3 mmol, 1.0 M equivalent) was dissolved in water (10 mL) and a catalytic amount of Pd/C (ca 5 mg, 0.031 mmol, 0.1 M equivalent) was added. The mixture was vigorously stirred overnight at RT under H_2 (1 standard atmosphere). The mixture was filtered on a pad of celite to remove the catalyst. Water was evaporated under vacuum at 50 °C and the final product was recovered as a pale yellow solid. This was used for the next step without further purification (185 mg, 97% yield). Melting point: >350 °C. ^{1}H NMR (400 MHz, D_2O) δ 8.66 (d, J = 1.9 Hz, 1H), 8.48 (d, J = 2.0 Hz, 1H), 8.29 (d, J = 2.0 Hz, 1H), 8.18 (d, J = 1.9 Hz, 1H), 7.92 (d, J = 8.5 Hz, 2H), 7.65 (d, J = 8.5 Hz, 2H), 6.96 – 6.85 (m, 4H), 6.71 (dd, J = 7.6, 2.0 Hz, 1H). ^{13}C NMR (101 MHz, D_2O) δ 168.4, 167.7, 146.3, 141.6, 140.7, 139.1, 138.8, 135.2, 133.4, 131.9, 129.2, 128.9, 128.7, 126.6, 126.2, 125.0, 124.7, 120.5, 119.9, 117.7, 114.3. IR νmax /cm-1: 3466 (OH), 1646, 1595, 1525 (C—H, aromatic sp2 stretch) cm^{-1}. HRMS (nESI-LTQ Orbitrap XL) *m/z*: $[M-2H]^{2-}$ calculated for $C_{24}H_{17}N_3O_{11}S_3$, 309.5018; found, 309.5018.

8-(4-[3-(([3-((4-[(3,6,8-trisulfonaphthalen-1-yl)carbamoyl] phenyl)carbamoyl)phenyl] cabamoyl)amino)benzamido] benzamido)naphthalene-1,3,6-trisulfonic acid (6). 8-[4-(3-Aminobenzamido)benzamido]naphthalene-1,3,6-trisulfonic acid **(14)** (250 mg, 0.4 mmol, 1.0 M equivalent) was dissolved in water (3 mL) and the pH was adjusted to 6–7 by adding Na_2CO_3 (1 M). To this mixture, a solution of triphosgene (60 mg, 0.2 mmol, 0.5 M equivalent) in toluene (3 mL) was added dropwise. The reaction was vigorously stirred for 8 h at RT. During this time the pH was regularly checked and adjusted to 6–7 by adding Na_2CO_3 (1 M). The water phase was extracted with EtOAc (3

× 5 mL). The water was evaporated under reduced pressure at 50 °C affording a pale yellow solid (200 mg, 39% yield). Melting point: >350 °C. ^{1}H NMR (400 MHz, D_2O) δ 8.51 (d, J = 2.1 Hz, 2H), 8.37 (d, J = 2.1 Hz, 1H), 8.27 (s, 1H), 8.21 – 8.13 (m, 3H), 7.86 (d, J = 8.5 Hz, 2H), 7.36 (d, J = 7.6 Hz, 1H), 7.13 (t, J = 7.9 Hz, 1H), 6.49 (d, J = 7.9 Hz, 1H). IR νmax /cm^{-1}: 3437 (OH), 1645, 1610, 1525 (C—H, aromatic sp2 stretch) cm^{-1}. HRMS M = $C_{49}H_{32}N_6O_{23}S_6Na_4$, then $[M-2H]^{(2-)}$ expected 676.9644; found 676.9643.

3.2.3. Synthesis of 7

8-[3-(4-nitrobenzamido)benzamido] naphthalene-1,3,6-trisulfonic acid (12). To 8-(3-Aminobenzamido)naphthalene-1,3,6-trisulfonic acid **(9)** (680 mg, 1.4 mmol, 1.0 M equivalent), water (5 mL) was added and the pH was adjusted to pH 6–7. To this, 4-nitro benzoyl chloride (351 mg, 1.9 mmol) dissolved in toluene (5 mL) was added. The reaction was stirred vigorously over a period of 8 h while the pH was continually adjusted to pH 6–7. The toluene layer was removed and the aqueous layer was acidified to pH 3 and extracted with EtOAc (3 × 10 mL). The remaining aqueous layer was evaporated to dryness to give the product as an orange solid powder (800 mg, 87% yield). ^{1}H NMR (400 MHz, D_2O) δ 8.50 (d, J = 1.9 Hz, 1H), 8.19 (d, J = 2.0 Hz, 1H), 8.04 (d, J = 2.0 Hz, 1H), 7.99 (d, J = 1.8 Hz, 1H), 7.82 (d, J = 2.1 Hz, 1H), 7.56 (d, J = 7.7 Hz, 1H), 7.38 – 7.29 (m, 4H), 7.15 – 7.09 (m, 1H), 7.01 (t, J = 7.8 Hz, 1H). ^{13}C NMR (101 MHz, D_2O) δ 166.2, 165.2, 147.4, 140.6, 139.1, 138.5, 138.4, 137.6, 134.9, 134.5, 132.6, 131.7, 131.15, 129.6, 128.4, 127.9, 126.2, 124.9, 123.9, 123.5, 123.1, 122.7, 122.4, 119.1. IR νmax /cm^{-1}: 3445 (OH), 1651, 1595 and 1524 (C—H, aromatic sp2 stretch). HRMS (nESI-LTQ Orbitrap XL) m/z $[M-2H]^{2-}$ calculated for $C_{24}H_{15}N_3O_{13}S_3$, 324.4889; found, 324.4886.

8-[3-(4-aminobenzamido)benzamido] naphthalene-1,3,6-trisulfonic acid (15). 8-[3-(4-Nitrobenzamido)benzamido]naphthalene-1,3,6-trisulfonic acid **(12)** (500 mg, 0.76 mmol, 1.0 M equivalent) was dissolved in water (10 mL) and a catalytic amount of Pd/C (ca 50 mg, 0.1 M equivalent) was added. The mixture was vigorously stirred overnight at RT under H_2 (1 standard atmosphere). The mixture was filtered over a pad of celite to remove remaining catalyst. The water was evaporated under reduced pressure at 50 °C to give the final product as a fine yellow powder, (450 mg, 94% yield). ^{1}H NMR (400 MHz, D_2O) δ 8.76 (s, 1H), 8.64 (s, 1H), 8.44 (s, 1H), 8.30 (s, 1H), 8.09 (s, 1H), 7.77 (dd, J = 22.2, 7.9 Hz, 2H), 7.53 (d, J = 8.1 Hz, 3H), 6.58 (d, J = 8.2 Hz, 2H). ^{13}C NMR (101 MHz, D_2O) δ 168.5, 168.3, 150.8, 140.8, 139.3, 138.9, 137.9, 135.1, 133.9, 132.1, 131.9, 129.4, 129.1, 126.7, 126.4, 125.8, 125.5, 125.1, 124.2, 122.3, 120.7, 114.76. IR νmax /cm^{-1}: 3404 (OH), 1605, 1512 (C—H, aromatic sp2 stretch). HRMS M = $C_{24}H_{19}N_3O_{11}S_3$ $[M+H]^{(+)}$ expected 622.0254; found 622.0232.

8-(3-[4-([4-((3-[(3,6,8-trisulfonaphthalen-1-yl)carbamoyl] phenyl)carbamoyl)phenyl] carbamoyl)amino)benzamido] benzamido)naphthalene-1,3,6-trisulfonic acid (7). 8-[3-(4-Aminobenzamido)benzamido]naphthalene-1,3,6-trisulfonic acid **15** (200 mg, 0.32 mmol) was dissolved in water (3 mL) and the pH was adjusted to 6–7 by adding Na_2CO_3 (1 M). To this mixture, a solution of triphosgene (47 mg, 0.16 mmol) in toluene (3 mL) was added dropwise. The reaction was vigorously stirred for 8 h at RT, with the pH regularly adjusted to 6–7 by adding Na_2CO_3 (1 M). The water phase was extracted with EtOAc (3 × 10 mL). The water was evaporated under reduced pressure at 50 °C affording a pale yellow solid (126 mg, 31% yield). Melting point: 330–332 °C. ^{1}H NMR (400 MHz, D_2O) δ 8.66 (d, J = 2.0 Hz, 1H), 8.47 (d, J = 1.9 Hz, 1H), 8.34 (d, J = 1.9 Hz, 1H), 8.23 (d, J = 1.9 Hz, 1H), 7.94 (s, 1H), 7.71 (d, J = 7.7 Hz, 1H), 7.53 (d, J = 8.2 Hz, 1H), 7.48 (d, J = 8.4 Hz, 2H), 7.36 (t, J = 7.9 Hz, 1H), 7.06 (d, J = 8.3 Hz, 2H). ^{13}C NMR (101 MHz, D_2O) δ 168.42, 167.1, 152.4, 141.7, 140.8, 139.3, 138.7, 137.7, 134.9, 133.8, 132.05, 131.8, 129.8, 128.4, 126.8, 126.5, 126.5, 125.5, 125.3, 123.9, 120.6, 117.9. IR νmax /cm^{-1}: 3447 (OH), 1593, 1526 and 1482 (C—H, aromatic sp2 stretch). HRMS (nESI-LTQ Orbitrap XL) m/z: $[M-5H]^{5-}$ calculated for $C_{49}H_{31}O_{23}N_6S_6$, 252.5958; found, 252.5960.

3.2.4. Synthesis of 16

4-[2-(2-{2-[2-(4-carboxyphenoxy)ethoxy] ethoxy)ethoxy] benzoic acid (17). To a round bottomed-flask (100 mL) tetraethylene glycol di(p-toluenesulfonate) (1.0 g, 2.0 mmol), ethyl p-hydroxybenzoate (600 mg, 3.6 mmol) and sodium hydroxide (160 mg, 1.5 mmol) were added. The reaction was purged under N_2 for 10 min and then IPA (15 mL) was added. The reaction was refluxed overnight and a white precipitate was produced. This precipitate was filtered and the filtrate was concentrated under reduced pressure to give a clear oil. The oil was mixed with a 10% NaOH w/v solution prepared in EtOH (15 mL) and refluxed for 1 h. The solvent was removed and the solid white material was dissolved in water (30 mL) and acidified to pH 3 to give a white precipitate. This was collected by vacuum filtration and dried in a desiccator overnight. The material was recrystallized from EtOH to give a fluffy white powder (377 mg, 43% yield). Melting point: 184–186 °C. ^{1}H NMR (400 MHz, DMSO-d_6) δ 12.62 (s, 1H), 7.88 (d, J = 8.8 Hz, 2H), 7.02 (d, J = 8.8 Hz, 2H), 4.15 (dd, J = 5.7, 3.5 Hz, 2H), 3.81 – 3.72 (m, 2H), 3.67 – 3.33 (m, 4H). ^{13}C NMR (101 MHz, DMSO-d_6) δ 167.4, 162.5, 131.8, 123.5, 114.7, 70.4, 70.3, 69.2, 67.9. IR νmax /cm^{-1}: 3400 (OH), 1661, 1605 and 1578 (C—H, aromatic sp2 stretch). HRMS M = $C_{22}H_{26}O_9$ $[M-H]^{(-)}$ expected 433.1504; found 43.1524.

8-[4-(2-{2-[2-(2-{4-[(3,6,8-trisulfonaphthalen-1-yl)carbamoyl] phenoxy)ethoxy)ethoxy] ethoxy)ethoxy)benzamido] naphthalene-1,3,6-trisulfonic acid (16). To 4-[2-(2-{2-[2-(4-carboxyphenoxy)ethoxy]ethoxy)ethoxy)ethoxy]benzoic acid **17** (100 mg, 0.23 mmol, 1.0 M equivalent), anhydrous dichloromethane (10 mL) was added under an atmosphere of N_2. Oxalayl chloride (300 μL, 3.45 mmol, 15 M equivalent) was added dropwise and the reaction was refluxed for 3 h until a yellow solution was observed. The dichloromethane layer was removed under reduced pressure. The crude material was re-dissolved in toluene (2 mL) and 8-amino-1,3,6-trisulfonic acid (153 mg, 0.4 mmol, 2.0 M equivalent) dissolved in water (2 mL) was added dropwise and pH regularly corrected to 6–7. The reaction was left for 2 h, after which the pH no longer became acidic, and the aqueous layer was recovered and evaporated to dryness to yield yellow crystals (20 mg, 7% yield). Melting point: 322–324 °C. ^{1}H NMR (400 MHz, D_2O) δ 8.58 (d, J = 2.1 Hz, 2H), 8.44 (d, J = 2.1 Hz, 2H), 7.82 (d, J = 2.0 Hz, 2H), 7.78 (d, J = 9.0 Hz, 2H), 7.34 (d, J = 2.0 Hz, 2H), 6.92 (d, J = 8.8 Hz, 2H), 4.13 – 4.09 (m, 4H), 3.79 – 3.75 (m, 4H), 3.65 – 3.56 (m, 8H). ^{13}C NMR (101 MHz, D_2O) δ 175.2, 160.4, 144.6, 141.7, 139.5, 138.7, 135.7, 131.8, 130.9, 129.1, 124.7, 120.18, 117.1, 114.1, 111.3, 69.6, 69.5, 68.9, 67.1. IR νmax /cm^{-1}: 3391 (OH), 1634, 1539 (C—H, aromatic sp2 stretch). Precursor **17** was detected in MS, indicating potential cleavage of amide bonds during analysis. HRMS M = $C_{22}H_{26}O_9$ $[M-H]^{(-)}$ expected 433.1504; found 433.1511.

3.3. Cell and explant culture

HTB94 human chondrosarcoma cells (American Culture Type Collection) were maintained at 37 °C and 5% CO_2 in a humidified incubator in Dulbecco's modified Eagle's medium (DMEM, Lonza) with 10% fetal calf serum (FCS, Merck), 100 U penicillin and 100 U streptomycin (Lonza). Cells were passaged using a mixture of 0.5 g/L trypsin and 0.2 g/L EDTA (Lonza).

Porcine cartilage explants were dissected from metacarpophalangeal joints of 3- to 9-month-old pigs within 24 h of euthanasia at an abattoir, and maintained in 6-well plates in cartilage growth media (DMEM containing 2 mg/mL amphotericin B, 10 mM HEPES, 100 U penicillin and 100 U streptomycin) with 10% FCS at 37 °C in 5% CO_2. Explants were rested for 48 h after dissection before further use.

Chondrocyte were isolated from freshly-dissected porcine cartilage explants by incubation with pronase E (Merck, 0.05% in serum-free cartilage growth media, 2 h, 37 °C), followed by type II collagenase (ThermoFisher, 0.075% in cartilage growth media containing 10% FCS, 18 h, 37 °C). Cells were strained through a 70 μm strainer and washed in PBS twice before plating in cartilage growth media containing 10% FCS.

3.4. Preparation of RAP

Receptor-associated protein (RAP) was expressed in *E. coli* and purified as described previously[37].

3.5. Quantification of TIMP-3 in conditioned media

HTB94 cells (5x10^5 per well) were plated overnight into 6-well plates in DMEM with 10% FCS, and washed three times with serum-free DMEM (DMEM containing 100 U penicillin and 100 U streptomycin) before treatment with suramin analogues (10–250 μg/mL) or other indicated reagents in 1.5 mL serum-free DMEM for 36 h.

For western blotting analysis of TIMP-3, conditioned media were concentrated by addition of 5% trichloroacetic acid (TCA, Merck, 4 °C, 18 h) and centrifugation (13 000 rpm, 4 °C, 15 min) to collect precipitated proteins. Pellets were resuspended in non-reducing sodium dodecyl sulfate (SDS) sample buffer (100 mM Tris.HCl, pH 6.8, 2% SDS, 15% glycerol, 0.1% bromophenol blue) and electrophoresed on 15% polyacrylamide gels, before transfer onto Immobilon-FL polyvinylidene fluoride (PVDF, Merck) membranes using the Trans-Blot Turbo transfer system (Bio-Rad).

For slot blot analysis of TIMP-3, TCA-concentrated media were applied directly to nitrocellulose membranes (Bio-Rad) by vacuum suction using a Hoefer PR 600 slot blotting manifold connected to a vacuum pump.

PVDF and nitrocellulose membranes were then incubated in Intercept blocking buffer (LI-COR, 1 h, 25 °C) and washed (4x5 min, 25 °C) in Tris-buffered saline (TBS) containing 0.1% (v/v) Tween 20 (ThermoFisher Scientific) between each subsequent step. TIMP-3 was detected by incubation of the blots with rabbit anti-TIMP-3 primary antibody [AB6000, Millipore, 1:1000 dilution in 50% Intercept buffer in TBS with 0.2 % (v/v) Tween 20, 18 h, 4 °C], followed by incubation with donkey anti-rabbit IgG coupled with IRDye 800CW [LI-COR, 1:4000 dilution in 50% Intercept in TBS with 0.2 % (v/v) Tween 20 and 0.02 % (m/v) SDS, 1 h, 25 °C]. Blots were imaged and quantified using an Odyssey CLx imaging system (LI-COR) and Image Studio version 4 software (LI-COR). TIMP-3 in the medium (mean ± SD, n = 3–6) was calculated relative to pixel volume in samples that were treated with 100 μg/mL suramin and analysed in parallel on each blot (defined as 100 %). EC_{50} values were calculated using a one-site specific binding model in Prism 9 for macOS (GraphPad Software).

3.6. Assessment of cell viability

HTB94 chondrosarcoma cells or primary porcine chondrocytes (10^4 per well) were plated overnight into 96-well plates in DMEM with 10% FCS, and washed three times with serum-free DMEM (100 U/mL P/S) before treatment with suramin analogues (100 μg/mL), RAP (1 μM) and/or interleukin 1β (10 ng/mL, Peprotech) in 200 μL serum-free DMEM for 36 h. As a control, cells in a parallel cell culture plate were twice frozen at −80 °C and thawed. Viability was then assessed using MTS (CellTiter 96 One Solution Cell Proliferation Assay, Promega) according to the manufacturer's instructions.

3.7. RT-qPCR evaluation of gene expression

HTB94 cells (5x10^5 per well) were plated overnight into 6-well plates in DMEM with 10 % FCS, and washed three times before treatment with suramin analogues (50–200 μg/mL) in 1.5 mL serum-free DMEM for 36 h. RNA was isolated from cells using an RNeasy kit (Qiagen) according to the manufacturer's instructions, including the optional treatment with DNase I (RNase-Free DNase Set, Qiagen). RNA was reverse transcribed to cDNA using a High Capacity cDNA Synthesis kit (Applied Biosystems) according to the manufacturer's instructions. Levels of *TIMP3*, *LRP1* and *18S* mRNA were quantified by RT-qPCR using a QuantStudio 5 (Applied Biosystems), with SyGreen Mix (PCRBIO) and KiCqStart SYBR Green primers (Merck). Primers (shown 5′ to 3′) for *TIMP3* were *CATGTGCAGTACATCCATAC* (forward) and *AGGTGATACCGATAGTTCAG* (reverse), for *LRP1* were *ACATATAGCCTCCATCCTAATC* (forward) and *GCTTATACCAGAATACCACTC* (reverse), for *MMP13* were *AAAGGGAATAAGTACTGGC* (forward) and *CAGTGTTTTCCTCAGAAAGAG* (reverse); for *ADAMTS4* were *AGAAGAAGTTTGACAAGTGC* (forward) and *CACATTGTTGTATCCGTACC* (reverse); for *ADAMTS5* were *CCCACCCAATGGTAAATC* (forward) and *GACTCCTTTTGCATCAGAC* (reverse); and for *RN18S1* were *ATCGGGGATTGCAATTATTC* (forward) and *CTCACTAAACCATCCAATCG* (reverse). Specificity of amplification was confirmed for all primer pairs by melt curve analysis of qPCR products. Fold changes were calculated in relation to the levels of *RN18S1* expression, using the ΔΔCt method.

3.8. Analysis of cartilage extracellular matrix degradation

Cartilage explants were washed three times with serum-free DMEM before treatment with IL-1β (10 ng/mL, Peprotech) and/or suramin analogues (100 μg/mL) in 1.5 mL DMEM containing 0.1% FCS, 2 mg/mL amphotericin B, and 10 mM HEPES for 72 h. Media were harvested and aggrecan release quantified using the DMMB dye binding assay[29].

3.9. Statistical analysis

Data were analysed by one- or two-way ANOVA in GraphPad Prism version 9 (GraphPad Software, La Jolla, CA). Data are shown as mean ± SD, with all significant changes annotated in the figures.

Declaration of Competing Interest

The authors declare that they have no known competing financial interests or personal relationships that could have appeared to influence the work reported in this paper.

Data availability

Data will be made available on request.

Acknowledgements

We would like to thank Dr S. F. Clarke from Cresset for his help with using the Flare software for computational evaluation of the analogues and the National Mass Spectrometry Facility at Swansea University for chemical analysis. We are grateful to Marco M. D. Cominetti for assistance with preparation of figures.

Author contributions

The manuscript was written through contributions of all authors. All authors have given approval to the final version of the manuscript.

Funding Sources

This research was funded by Versus Arthritis (grant number 21776).

Appendix A. Supplementary data

Supplementary data to this article can be found online at https://doi.org/10.1016/j.bmc.2023.117424.

References

1 Kloppenburg M, Berenbaum F. Osteoarthritis year in review 2019: epidemiology and therapy. *Osteoarthritis Cartilage*. 2020;28:242–248. https://doi.org/10.1016/j.joca.2020.01.002.
2 Hunter DJ, Bierma-Zeinstra S. Osteoarthritis. *Lancet*. 2019;393:1745–1759. https://doi.org/10.1016/S0140-6736(19)30417-9.

3 Little CB, Barai A, Burkhardt D, et al. Matrix metalloproteinase 13-deficient mice are resistant to osteoarthritic cartilage erosion but not chondrocyte hypertrophy or osteophyte development. *Arthritis Rheum*. 2009;60:3723–3733. https://doi.org/10.1002/ART.25002.

4 Stanton H, Rogerson FM, East CJ, et al. ADAMTS5 is the major aggrecanase in mouse cartilage in vivo and in vitro. *Nature*. 2005;434:648–652. https://doi.org/10.1038/nature03417.

5 Glasson SS, Askew R, Sheppard B, et al. Deletion of active ADAMTS5 prevents cartilage degradation in a murine model of osteoarthritis. *Nature*. 2005;434:644–648. https://doi.org/10.1038/nature03369.

6 Gendron C, Kashiwagi M, Hughes C, Caterson B, Nagase H. TIMP-3 inhibits aggrecanase-mediated glycosaminoglycan release from cartilage explants stimulated by catabolic factors. *FEBS Lett*. 2003;555:431–436. https://doi.org/10.1016/S0014-5793(03)01295-X.

7 Black RA, Castner B, Slack J, et al. Injected TIMP-3 protects cartilage in a rat meniscal tear model. *Osteoarthr Cartil*. 2006;14:S23-24. doi:10.1016/S1063-4584(07)60467-1.

8 Sahebjam S, Khokha R, Mort JS. Increased collagen and aggrecan degradation with age in the joints of Timp3-/- mice. *Arthritis Rheumatol*. 2007;56:905–909. https://doi.org/10.1002/art.22427.

9 Morris KJ, Cs-Szabo G, Cole AA. Characterization of TIMP-3 in human articular talar cartilage. *Connect Tissue Res*. 2010;51:478–490.

10 Swingler TE, Waters JG, Davidson RK, et al. Degradome expression profiling in human articular cartilage. *Arthritis Res Ther*. 2009;11:R96. https://doi.org/10.1186/ar2741.

11 Scilabra SD, Troeberg L, Yamamoto K, et al. Differential regulation of extracellular tissue inhibitor of metalloproteinases-3 levels by cell membrane-bound and shed low density lipoprotein receptor-related protein 1. *J Biol Chem*. 2013;288:332–342. https://doi.org/10.1074/jbc.M112.393322.

12 Troeberg L, Fushimi K, Khokha R, Emonard H, Ghosh P, Nagase H. Calcium pentosan polysulfate is a multifaceted exosite inhibitor of aggrecanases. *FASEB J*. 2008;22:3515–3524. https://doi.org/10.1096/fj.08-112680.

13 Yu WH, Yu SSC, Meng Q, Brew K, Woessner JF. TIMP-3 binds to sulfated glycosaminoglycans of the extracellular matrix. *J Biol Chem*. 2000;275:31226–31232. https://doi.org/10.1074/jbc.M000907200.

14 Lee MH, Atkinson S, Murphy G. Identification of the extracellular matrix (ECM) binding motifs of tissue inhibitor of metalloproteinases (TIMP)-3 and effective transfer to TIMP-1. *J Biol Chem*. 2007;282:6887–6898. https://doi.org/10.1074/jbc.M610490200.

15 Troeberg L, Lazenbatt C, Anower-E-Khuda MF, et al. Sulfated glycosaminoglycans control the extracellular trafficking and the activity of the metalloprotease inhibitor TIMP-3. *Chem Biol*. 2014;21:1300–1309. https://doi.org/10.1016/j.chembiol.2014.07.014.

16 Chanalaris A, Doherty CM, Marsden BD, et al. Suramin inhibits osteoarthritic cartilage degradation by increasing extracellular levels of chondroprotective tissue inhibitor of metalloproteinases 3. *Mol Pharmacol*. 2017;92:459–468. https://doi.org/10.1124/mol.117.109397.

17 Voogd TE, Vansterkenburg EL, Wilting J, Janssen LH. Recent research on the biological activity of suramin. *Pharmacol Rev*. 1993;45:177–203.

18 Guns LA, Monteagudo S, Kvasnytsia M, et al. Suramin increases cartilage proteoglycan accumulation in vitro and protects against joint damage triggered by papain injection in mouse knees in vivo. *RMD Open*. 2017;3:e000604.

19 Prasad JM, Young PA, Strickland DK. High affinity binding of the receptor-associated protein D1D2 domains with the low density lipoprotein receptorrelated protein (LRP1) Involves bivalent complex formation: Critical roles of lysines 60 and 191. *J Biol Chem*. 2016;291:18430–18439. https://doi.org/10.1074/jbc.M116.744904.

20 Fisher C, Beglova N, Blacklow SC. Structure of an LDLR-RAP Complex Reveals a General Mode for Ligand Recognition by Lipoprotein Receptors. *Mol Cell*. 2006;22:277–283. https://doi.org/10.1016/j.molcel.2006.02.021.

21 Van Den Biggelaar M, Sellink E, Klein Gebbinck JWTM, Mertens K, Meijer AB. A single lysine of the two-lysine recognition motif of the D3 domain of receptor-associated protein is sufficient to mediate endocytosis by low-density lipoprotein receptor-related protein. *Int J Biochem Cell Biol*. 2011;43:431–440. https://doi.org/10.1016/j.biocel.2010.11.017.

22 Dolmer K, Campos A, Gettins PGW. Quantitative dissection of the binding contributions of ligand lysines of the receptor-associated protein (RAP) to the low density lipoprotein receptor-related protein (LRP1). *J Biol Chem*. 2013;288:24081–24090. https://doi.org/10.1074/jbc.M113.473728.

23 Doherty CM, Visse R, Dinakarpandian D, Strickland DK, Nagase H, Troeberg L. Engineered tissue inhibitor of metalloproteinases-3 variants resistant to endocytosis have prolonged chondroprotective activity. *J Biol Chem*. 2016;291:22160–22172. https://doi.org/10.1074/jbc.M116.733261.

24 Jentsch KD, Hunsmann G, Hartmann H, Nickel P. Inhibition of Human lmmunodeficiency Virus Type I Reverse Transcriptase by Suramin-related Compounds. *J Gen Virol*. 1987;68:2183–2192.

25 Kassack MU, Braun K, Ganso M, et al. Structure-activity relationships of analogues of NF449 confirm NF449 as the most potent and selective known P2X1 receptor antagonist. *Eur J Med Chem*. 2004;39:345–357. https://doi.org/10.1016/j.ejmech.2004.01.007.

26 Trapp J, Meier R, Hongwiset D, Kassack MU, Sippl W, Jung M. Structure-activity studies on suramin analogues as inhibitors of NAD+-dependent histone deacetylases (sirtuins). *ChemMedChem*. 2007;2:1419–1431. https://doi.org/10.1002/cmdc.200700003.

27 Braddock PS, Hu DE, Fan TP, Stratford IJ, Harris AL, Bicknell R. A structure-activity analysis of antagonism of the growth factor and angiogenic activity of basic fibroblast growth factor by suramin and related polyanions. *Br J Cancer*. 1994;69:890–898. https://doi.org/10.1038/bjc.1994.172.

28 Croci R, Pezzullo M, Tarantino D, et al. Structural bases of norovirus RNA dependent RNA polymerase inhibition by novel suramin-related compounds. *PLoS One*. 2014;9:e91765.

29 Farndale RW, Buttle DJ, Barrett AJ. Improved quantitation and discrimination of sulphated glycosaminoglycans by use of dimethylmethylene blue. *Biochim Biophys Acta*. 1986;883:173–177.

30 Chien CC, Liu JH. Optical Behaviors of Cholesteric Liquid-Crystalline Polyester Composites with Various Chiral Photochromic Dopants. *Langmuir ACS J Surf Colloids*. 2015;31:13410–13419. https://doi.org/10.1021/acs.langmuir.5b03201.

31 Dysart S, Utkina K, Stong L, et al. Insights from Real-World Analysis of Treatment Patterns in Patients with Newly Diagnosed Knee Osteoarthritis. 2021;14(2).

32 Rothenfluh DA, Bermudez H, O'Neil CP, Hubbell JA. Biofunctional polymer nanoparticles for intra-articular targeting and retention in cartilage. *Nat Mater*. 2008;7:248–254. https://doi.org/10.1038/nmat2116.

33 Hu HY, Lim NH, Ding-Pfennigdorff D, et al. DOTAM Derivatives as Active Cartilage-Targeting Drug Carriers for the Treatment of Osteoarthritis. *Bioconjug Chem*. 2015;26:383–388. https://doi.org/10.1021/bc500557s.

34 Fowkes MM, Das Neves Borges P, Cacho-Nerin F, Brennan PE, Vincent TL, Lim NH. Imaging articular cartilage in osteoarthritis using targeted peptide radiocontrast agents. *PLoS One*. 2022;17:e0268223.

35 Pi Y, Zhang X, Shi J, et al. Targeted delivery of non-viral vectors to cartilage in vivo using a chondrocyte-homing peptide identified by phage display. *Biomaterials*. 2011;32:6324–6332. https://doi.org/10.1016/j.biomaterials.2011.05.017.

36 Pi Y, Zhang X, Shao Z, Zhao F, Hu X, Ao Y. Intra-articular delivery of anti-Hif-2α siRNA by chondrocyte-homing nanoparticles to prevent cartilage degeneration in arthritic mice. *Gene Ther*. 2015;22:439–448. https://doi.org/10.1038/gt.2015.16.

37 Yamamoto K, Troeberg L, Scilabra SD, et al. LRP-1-mediated endocytosis regulates extracellular activity of ADAMTS-5 in articular cartilage. *FASEB J*. 2013;27:511–521. https://doi.org/10.1096/fj.12-216671.